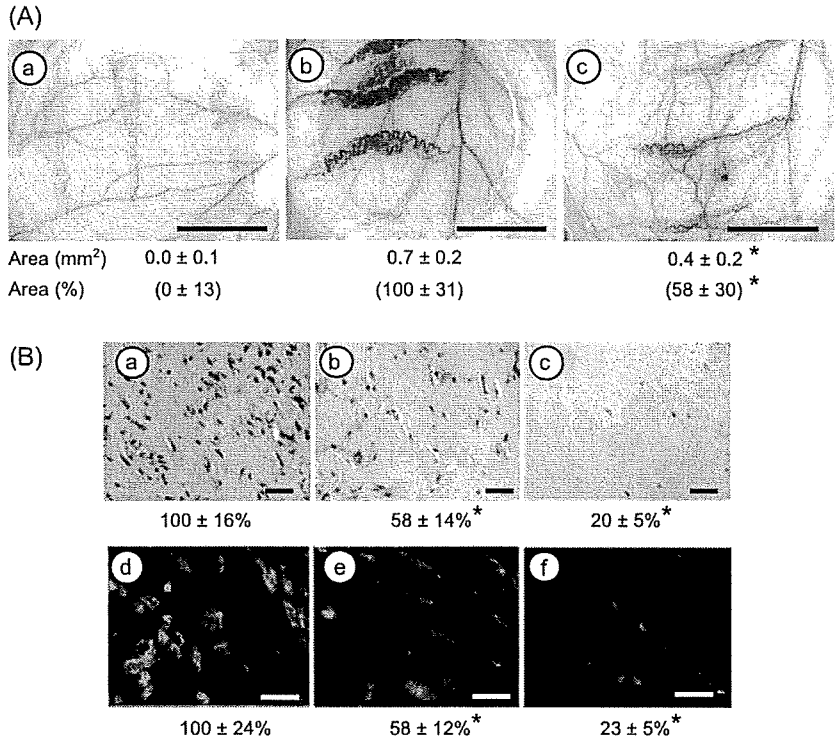

Fig. 3. Suppression of tumor-induced and vascular endothelial growth factor (VEGF)-induced *in vivo* angiogenesis by β-hydroxyisovalerylshikonin (β-HIVS) in dorsal air sac (DAS) and Matrigel plug assay. (A) DAS assay, chambers filled with either medium alone (a) or Lewis lung carcinoma (LLC) cells (b,c) were implanted into 7-week-old mice. Aliquots (100 μL) of vehicle or β-HIVS (30 mg/kg bodyweight) were injected i.p. every other day for 3 days starting at 1 day after implantation (b and c, respectively). The next day the dorsal skin was peeled off and blood vessel formation was examined under a microscope and photographed. Representative micrographs from six mice in each group are shown. Scale lines, 5 mm. Areas of tumor-induced blood vessels were analyzed with angiogenesis-measuring software and these areas are given under each photograph. Relative areas are given as percentages in parentheses. Values represent average ± standard deviation ($n = 6$). An asterisk represents a significant difference ($P < 0.05$) from the results obtained with the vehicle alone. (B) Matrigel plug assay, Matrigel plugs containing 50 ng/mL VEGF ± 5 μM or 10 μM β-HIVS were implanted into mice s.c. One week later, the Matrigel plugs were collected and stained with hematoxylin–eosin (a–c) and platelet/endothelial cell adhesion molecule-1 (PECAM-1)-specific antibody (d–f). (a,d) VEGF alone (control); (b,e) VEGF plus 5 μM β-HIVS; (c,f) VEGF plus 10 μM β-HIVS. Representative data from a total of nine micrographs (three fields × three mice) are presented. Scale lines, 100 μm. The number of invading cells in each micrograph was counted and the relative values are presented as percentages under each photograph. Values represent average ± standard error ($n = 9$, three fields × three mice). An asterisk indicates a significant difference ($P < 0.05$) from the control. (A,B) Representative results from two or three independent experiments that all gave similar results.

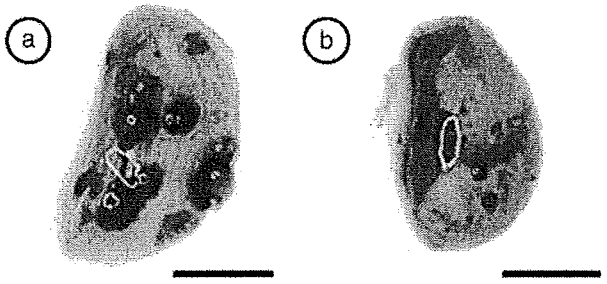

Fig. 4. Inhibition of tumor metastasis by β-hydroxyisovalerylshikonin (β-HIVS). The effect of β-HIVS on metastasis of Lewis lung carcinoma (LLC) cells was assessed as described in Materials and Methods. (a) Vehicle; (b) β-HIVS. Representative photographs from a total of five mice are shown. Relative changes in colonies of metastatic tumor cells are shown as a percentage of control in parenthesis. Scale lines, 5 mm. Values are mean ± standard deviation ($n = 5$). An asterisk indicates a significant difference ($P < 0.05$) from the control group. A representative result from two independent experiments that gave similar results is shown.

using a combination of LipofectAMINE Plus regent (Invitrogen) and a GC3-Luc vector (500 ng/dish), which was constructed by inserting a synthesized oligodeoxynucleotide cassette corresponding to three sequential repeats of the GC box motifs and TATA box upstream of the luciferase cDNA of the pGL3 vector (Promega, Madison, WI, USA), or Tie2-luc vector (500 ng/dish).[17] On the day after the transfection, the cells were washed, and treated with 5 μM β-HIVS in a medium containing 2.5% serum for 10 h, and luciferase activity of the cells was determined as before.[16]

doi: 10.1111/j.1349-7006.2008.01049.x

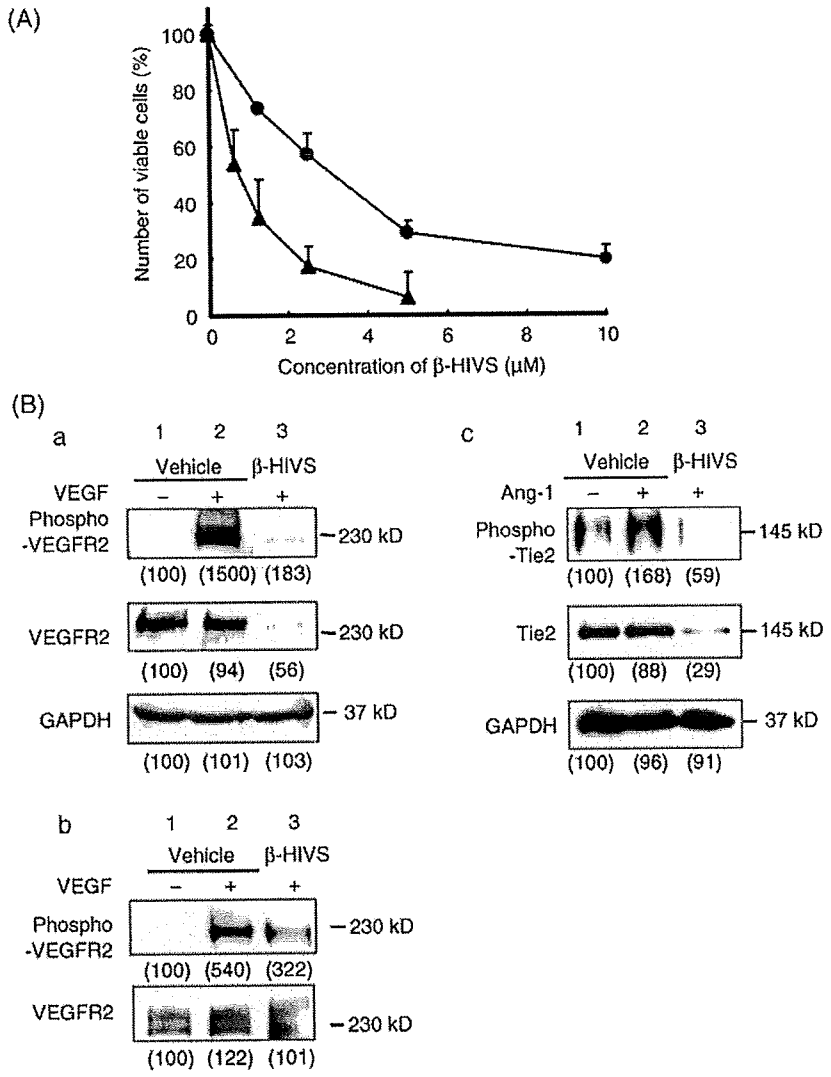

Fig. 5. Suppression by β-hydroxyisovaleryl-shikonin (β-HIVS) of vascular endothelial and progenitor cell growth accompanying reduced phosphorylation and expression of vascular endothelial growth factor receptors (VEGFR)2 and Tie2. (A) One day after human umbilical vein endothelial cells (HUVEC) or vascular progenitor cells (VPC; 1×10^5 cells) had been seeded onto 3.5-cm dishes, they were incubated for 24 h in growing medium that contained 50 ng/mL vascular endothelial growth factor (VEGF) and increasing concentrations of β-HIVS. Cells were stained with Trypan blue, and numbers of unstained viable cells were counted and plotted as percentages relative to values for untreated control cells (1.7×10^5 cells in a 3.5-cm dish). Values represent mean ± standard deviation ($n = 3$) (●) HUVEC; (▲) VPC. (B) After HUVEC and NIH-3T3-VEGFR2 cells had been incubated for 24 h with or without 5 μM β-HIVS in medium containing 2.5% serum, cells were stimulated with either 50 ng/mL VEGF (a,b), or 100 ng/mL Ang-1 (c) for 5 min, and then lyzed immediately. The amount of each phosphorylated receptor (upper panels) as well as the total amount of each receptor (middle panels) and glyceraldehyde 3-phosphate dehydrogenase (GAPDH, a loading control; lower panels) were assessed as described in Materials and Methods. (A,B) Representative results from three independent experiments that all gave similar results.

Statistical analysis. Data are expressed as mean ± standard deviation or ± standard error. Statistical significance was assessed by one-way ANOVA followed by Scheffe's Student's *t*-test.

Results

Inhibition of the blood vessel formation in CAM by β-HIVS. The effect of β-HIVS and shikonin on *in vivo* angiogenesis was examined in the CAM assay (Fig. 2A). The formation of intricate vascular networks, developing within control CAM (Fig. 2A,a), was moderately suppressed with shikonin at a concentration of 720 ng/egg (250 μM inside the ring, Fig. 2A,d), whereas β-HIVS exerted much stronger anti-angiogenic activity in a dose-dependent manner at concentrations of 9.7–970 ng/egg (corresponding to 2.5–250 μM inside the ring, Fig. 2A,e–g) (the actual concentrations of shikonin and β-HIVS within CAM tissues were lower than these concentrations due to diffusion of the drug). Treatment with 250 μM β-HIVS inhibited angiogenesis with CAM by 50%, more efficiently than 29% with 250 μM shikonin. The result of plotting the inhibition curve suggested that β-HIVS is a threefold more potent anti-angiogenic inhibitor than shikonin (Fig. 2B). Staining with hematoxylin–eosin of vertical sections of CAM tissues revealed that exposure to 250 μM β-HIVS for 48 h caused a 55% reduction in the number of capillaries that developed underneath the chorionic epithelium without affecting epithelial cells composing the chorionic membrane (Fig. 2C).

Suppression of *in vivo* angiogenesis by β-HIVS in DAS and matrigel plug assay. Figure 3A shows the result of DAS assays using murine LLC cells. From pre-existing blood vessels beneath the epidermis (Fig. 3A,a), strikingly disorganized and tortuous vessels were induced towards tumor cells in the chamber (Fig. 3A,b), which was reduced by 42% in mice administered β-HIVS at 30 mg/kg bodyweight (Fig. 3A,c). Under the same condition, the bodyweight of the mice with implanted chambers did not change significantly (data not shown). No obvious sign of toxicity in kidney vasculature and tracheal mucosa (Supplementary Fig. S1a,b) or proteinuria (Supplementary Fig. S2A) was observed in β-HIVS-administrated mice, while moderate damage was seen in the liver (Supplementary Fig. S1,f). To determine whether β-HIVS might act on blood vessel cells and inhibit blood vessel formation, we examined the effect of β-HIVS in the Matrigel plug assay (Fig. 3B). Invasion of cells was observed in the control Matrigel that contained VEGF without β-HIVS (Fig. 3B,a). When β-HIVS was administered in the Matrigel at a

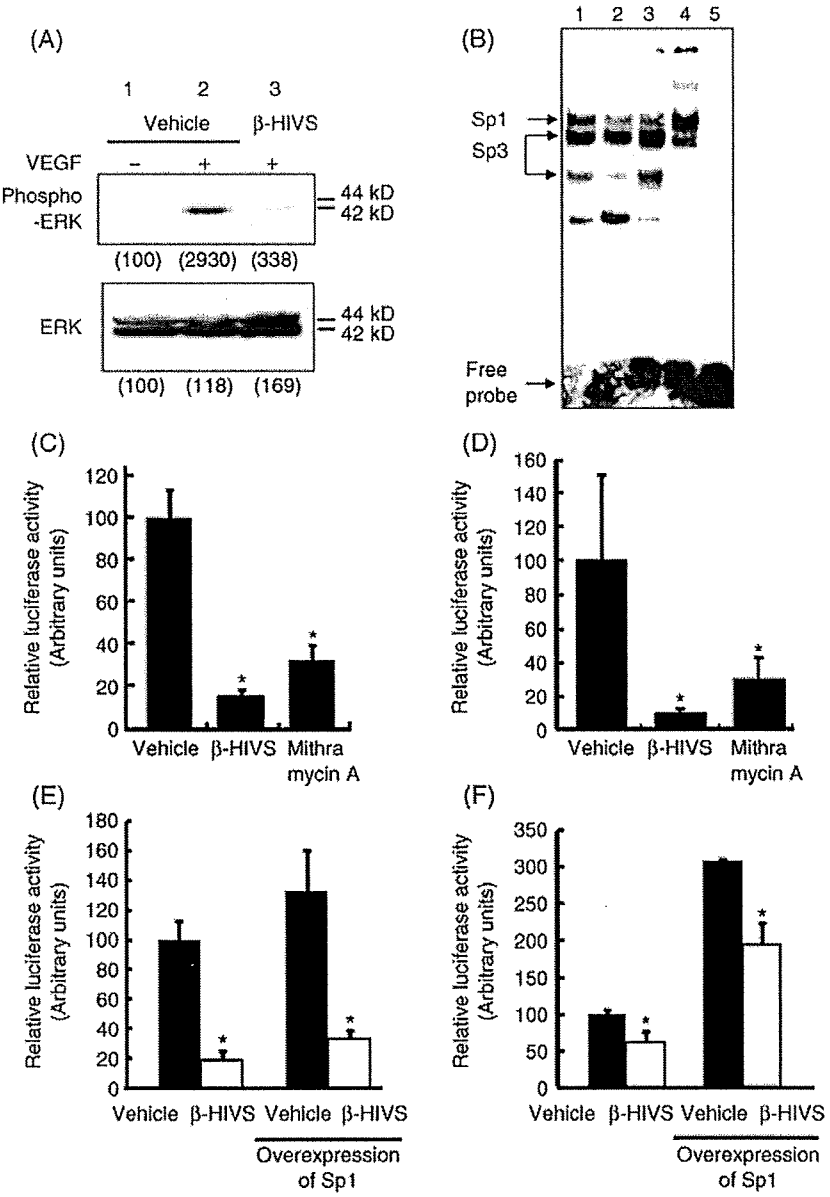

Fig. 6. Suppression in mitogen activated protein kinase (MAPK)-Sp1 pathway by β-hydroxyisovalerylshikonin (β-HIVS). (A) β-HIVS on the activation of externally regulated kinases (ERK). After human umbilical vein endothelial cells (HUVEC) had been incubated for 24 h with or without 5 μM β-HIVS in medium that contained 2.5% serum, cells were stimulated with 50 ng/mL vascular endothelial growth factor (VEGF) for 5 min, and cell lysates were prepared and subjected to western blot analysis. Upper panel, changes in phosphorylated ERK protein. Lower panel, changes in total amounts of ERK protein. (B) β-HIVS on Sp1 binding. After treatment of HUVEC with 5 μM β-HIVS for 24 h, nuclear extracts were prepared and Sp1 binding to the *VEGFR2* GC box motif was assessed by gel shift assay. Lane 1, vehicle; lane 2, 5 μM β-HIVS; lane 3, vehicle + anti-Sp1 immunoglobulin (Ig)G; lane 4, vehicle + Sp3 IgG; lane 5, vehicle + unlabeled oligonucleotide. (C) GC3 motif-luciferase reporter activity. Bovine aortic endothelial cells (BAEC) were transfected with a GC3 motif-luciferase chimeric gene construct. The day after transfection, the medium was changed and the cells were treated with 5 μM β-HIVS or 10 nM mithramycin A for 10 h. Transactivation activity was assessed by luciferase reporter assay and plotted as percentages of the values for the control (vehicle). (D) *Tie2* promoter-luciferase reporter activity. BAEC were transfected with a Tie2-luciferase chimeric gene construct. The day after transfection, the medium was changed and cells were treated with 5 μM β-HIVS or 10 nM mithramycin A for 10 h. Transactivation activity was assessed by luciferase reporter assay and plotted as percentages of the values for the control (vehicle). (E), (F) Partial rescue of β-HIVS's inhibition in GC3 motif-luciferase (E) and Tie2 promoter-luciferase (F) reporter activities with constitutively active MEK. BAECs were transfected with combinations of either a GC3 motif-luciferase (E) or a Tie2 promoter-luciferase (F) chimeric gene construct and empty vector or constitutively active MEK gene-expressing vector. The next day of transfection, medium was changed and cells were treated with 5 μM β-HIVS for 10 h. Transactivation activity was assessed as before, and plotted as percentages of the values for the control (vehicle). (A–F) Representative results from two or three independent experiments that all gave similar results. (C)–(F). Values represent means ± standard deviation ($n = 3$) Asterisks indicate significant differences ($P < 0.05$) from respective controls.

concentration of 5 μM, the VEGF-induced invasion of cells was inhibited by approximately 42% (Fig. 3B,b). More than 47% of the invading cells were platelet/endothelial cell adhesion molecule-1 immunopositive endothelial cells and/or the progenitor cells (Fig. 3B,a,d). No obvious sign of toxicity was observed in β-HIVS treated mice. These results suggested that β-HIVS suppressed tumor-induced blood vessel formation *in vivo*, at least in part, via a direct action on vascular endothelial and/or progenitor cells. Moreover, spontaneous metastasis of implanted LLC cells to the lung was suppressed to 46% by i.p. administration of β-HIVS (10 mg/kg bodyweight) for 3 weeks (Fig. 4). The bodyweight of the mice did not change significantly and only the weights of original tumor tissues were reduced by 46% (data not shown).

β-HIVS suppressed the phosphorylation and expression of both VEGFR2 and Tie2, and inhibited the growth of both vascular endothelial and progenitor cells. We investigated the molecular mechanism by which β-HIVS inhibited blood vessel formation via a direct effect on the vascular endothelial and/or progenitor cells. Simultaneous inclusion of VEGF and β-HIVS suppressed the proliferation of HUVEC and VPC in a dose-dependent manner, reducing their cell numbers to 20% at 10 μM and 2.5 μM (IC_{50}, 3 and 1 μM), respectively (Fig. 5A). We next examined whether β-HIVS could abrogate the growth stimulating and survival signals by inhibiting the phosphorylation of the angiogenic growth factor receptors in endothelial cells as implicated in the previous report using a reconstituted system in other cell types.[9] As seen in the upper panel of Figure 5(B,a), induction of phosphorylated 230 kDa VEGFR2 due to VEGF treatment was almost completely blocked by pretreatment with 5 μM β-HIVS for 24 h (compare Fig. 5B,a lanes 2 and 3). A similar result was observed with NIH3T3 cells that constitutively overexpressed VEGFR2 (Fig. 5B,b). Surprisingly, levels of VEGFR2 protein expression itself were also significantly reduced following β-HIVS-pretreatment (Fig. 5B,a lane 3 in middle panel). In addition, β-HIVS suppressed the phosphorylation

doi: 10.1111/j.1349-7006.2008.01049.x

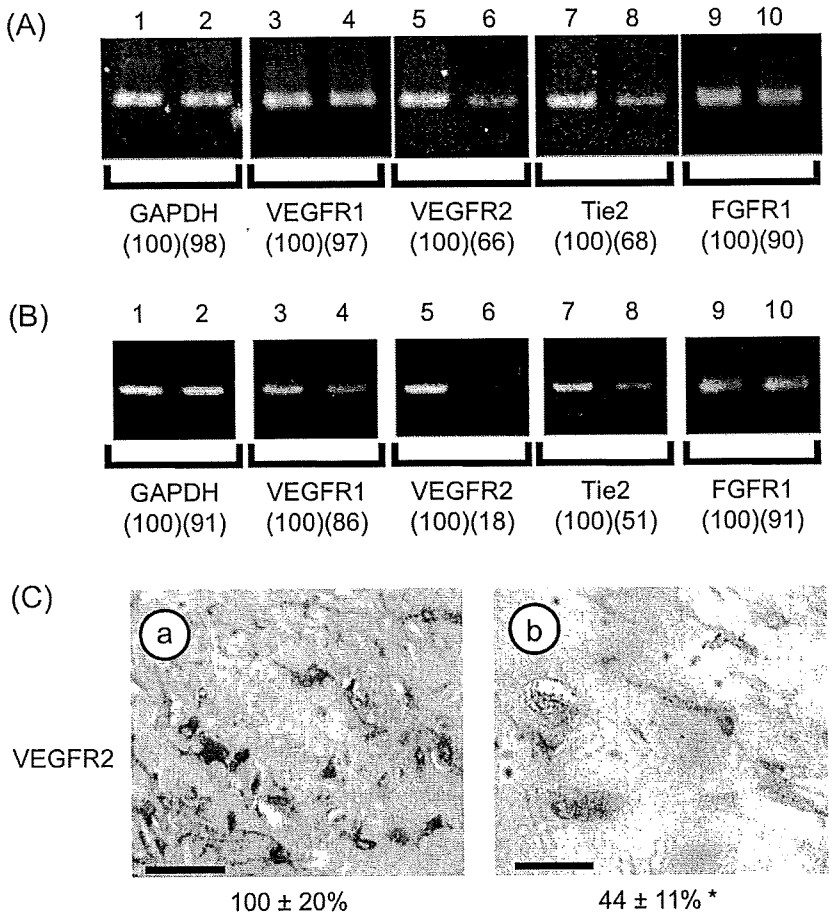

Fig. 7. Suppression of expression of vascular endothelial growth factor receptor (VEGFR) and Tie2 by β-hydroxyisovalerylshikonin (β-HIVS). (A) β-HIVS on mRNA levels of several growth factor receptors. Human umbilical vein endothelial cells (HUVEC) were treated for 24 h with 5 μM β-HIVS. Changes in mRNA levels of the indicated genes were assessed by reverse transcription polymerase chain reaction (RT-PCR). Relative changes in levels were calculated after normalization to levels of *GAPDH* mRNA and are presented as percentages in parentheses under each band. (B) 10 h after HUVEC were treated with 10 nM mithramycin A, changes in mRNA levels were determined by RT-PCR as before. Relative changes in levels were calculated after normalization to levels of *GAPDH* mRNA and are presented as percentages in parentheses under each band. (C) β-HIVS on VEGFR2 expression *in vivo*. Matrigel plugs containing 50 ng/mL vascular endothelial growth factor (VEGF) ± 5 μM β-HIVS were implanted s.c. into mice. A week later, the Matrigel plugs were collected and immunostained with VEGFR2. (a) Minus β-HIVS; (b) plus β-HIVS. Scale lines, 50 μm. The antigen-positive cells in each micrograph were counted and relative changes in numbers are presented as percentages under each photograph. Values represent average ± standard error ($n = 5$). An asterisk indicates a significant difference ($P < 0.05$) from the control. Representative data from a total of nine micrographs (three fields × three mice) are presented. (A–C) Representative results from two or three independent experiments that all gave similar results.

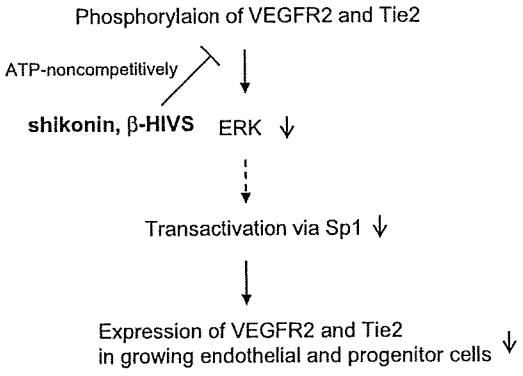

Fig. 8. Hypothetical molecular mechanism. Shikonin and β-hydroxyisovalerylshikonin (β-HIVS) suppress angiogenesis by inhibiting the phosphorylation of vascular endothelial growth factor receptor (VEGFR)2 and Tie2, subsequent inhibition of externally regulated kinases (ERK) and downstream Sp1, culminating in suppression of VEGFR2 and Tie2 expression. ATP, adenosine triphosphate.

and expression of Tie-2 (Fig. 5B,c lane 3 in upper and middle panels, respectively). Under the same condition, levels of GAPDH, an internal control, was unchanged (Fig. 5B, a and c, lane 3 in lower panels).

β-HIVS suppressed MAPK and Sp1-dependent expression of VEGFR2 and Tie2 mRNA. We next investigated the molecular mechanism by which β-HIVS reduced the expression of VEGFR2 and Tie2 in the further detail. β-HIVS abrogated cellular production of phospho-ERK (Fig. 6A lane 3 in upper panel) without changing the levels of total ERK themselves (Fig. 6A lane 3 in lower panel). It has been reported that Sp1 is a downstream transcription factor of ERK and transactivates the promoter of the *VEGFR2* gene.[18] Therefore, we next examined whether β-HIVS might suppress the expression of *VEGFR2* via reduction of Sp1 activity. Treatment of cells with β-HIVS lowered the Sp1 binding and transactivation activities toward the GC box motif within the *VEGFR2* gene promoter (Fig. 6B,C, respectively). β-HIVS also weakly inhibited binding activity of Sp3 transcription factor (Fig. 6B). Comparable reductions were observed in transactivation of the *Tie2* promoter (Fig. 6D) and in the expression of *VEGFR2* and *Tie2* mRNA (Fig. 7A), which were mimicked by mithramycin A, a specific inhibitor of the binding of Sp1/Sp3 to the GC box[19] (Figs 6D and 7B). Both β-HIVS and mithramycin A marginally affected mRNA levels of *VEGFR1* and *FGF receptor 1* (*FGFR1*) (Fig. 7A,B). Inhibition by β-HIVS was partially blocked by Sp1 over-expression in BAEC (Fig. 6E,F). β-HIVS also did not affect the levels of Sp1, VEGF, and Angs-1 and 2. Finally, suppression of the expression of VEGFR2 was also observed during the inhibition of angiogenesis *in vivo*, as assessed by immunostaining of the Matrigel plugs (Fig. 7C). In contrast to the large numbers of VEGFR2-positive cells in control Matrigel plugs (Fig. 7C,a), the number of VEGFR2-positive cells was reduced to 44 ± 11% of the control values (Fig. 7C,b) by inclusion of β-HIVS in the Matrigel plug at 5 μM.

Discussion

In this manuscript, we report the novel molecular mechanism, by which shikonins inhibit tumor angiogenesis. First, we found that β-HIVS exhibits much stronger anti-angiogenic activity than shikonin (Fig. 2A). We anticipate that an isovaleryl group present in the β-HIVS molecule will be found to play an important role in potentiating its anti-angiogenic action compared with that of shikonin. Administration of β-HIVS in mice weakly caused liver damage in the DAS (Supplementary Fig. S1,f), but not in the Matrigel plug assay (data not shown). β-HIVS did not affect epithelial cells constituting chorionic membrane in the CAM assay (Fig. 2B), vasculature in the kidney and tracheal mucosa (Supplementary Fig. S1,b,d), proteinuria (Supplementary Fig. S2A) and pre-existing blood vessels underneath the skin in DAS assay (Fig. 3A). These results suggest that the anti-angiogenic effect of β-HIVS may not be due to cytotoxic effects. Furthermore, neither cellular levels of GAPDH (Figs 5B and 7A) nor ERK (Fig. 6A) was affected by β-HIVS. These results suggest that it affects only proliferating cells that require growth factor stimuli. In Figure 3, because formation of new blood vessels was inhibited the number of platelet/endothelial cell adhesion molecule (PECAM)-negative non-endothelial cells such as macrophages were also thought to be reduced.

β-Hydroxyisovalerylshikonin appears to target the MAPK-Sp1 pathway (Figs 5 and 6) and downstream expression of VEGFR2 and Tie2, thereby inhibiting the growth of vascular endothelial and progenitor cells (Fig. 5A). This is consistent with previous reports that the Ras-MAPK signaling pathway plays an important regulatory role in angiogenesis,[20] and Sp1, a downstream transcription factor of ERK, transactivates the *VEGFR2* promoter.[15,21] On the other hand, the transactivation of *Tie2* promoter by Sp1 is a novel finding. The results in Fig. 6 definitely suggest a role of Sp1 in the expression of both *VEGFR2* and *Tie2*. In Fig. 6(B), lane 3, we could not see an obvious supershift of the Sp1 band, but saw diminishment in the Sp1 band. We think that this is because the anti-Sp1 immunoglobulin G we used for the supershift experiment competitively binds to Sp1's DNA binding domain and therefore that Sp1's bind diminished instead of being uppershifted. The suppressed expression in growth factor receptors is relatively selective for VEGFR2 and Tie2 (Fig. 7A). The effect would be dependent on cell type and experimental conditions. Combination of the current findings and what was reported previously[15,21] suggests that the primary target of β-HIVS is the phosphorylation of several tyrosine kinase receptors in vascular endothelial and/or progenitor cells, and as a secondary effect, the expression of VEGFR2 and Tie2 is suppressed due to reduced MAPK-Sp1 signaling (Fig. 8). It was recently reported that the autocrine VEGF/VEGFR2 signaling pathway is required for homeostasis of blood vessels.[22] Indeed, β-HIVS at higher concentrations (10 μM) induced apoptosis in vascular endothelial cells (Supplementary Fig. S3).

Both VEGF/VEGFR and Ang/Tie2 signaling pathways were important for tumor-associated angiogenesis[5,23] and vasculogenesis.[4] Several compounds have been shown to inhibit either the expression or the phosphorylation of VEGFR2.[24] Most of the clinically-used anti-angiogenic reagents are inhibitors that target VEGFR,[24] whereas a few angiogenesis inhibitors (all-*trans* retinoic acid and 3'-sulfoquinovosyl-1'-monoacylglycerol) have been reported to suppress the expression of Tie2.[12,25] Thus, anti-angiogenic activity targeting Tie2 has been drawing increased attention.[26,27] β-HIVS simultaneously suppressed both the expression and the phosphorylation of VRGFR2 as well as Tie2, suggesting that shikonins would be a novel leading compound to develop an anti-angiogenic reagent with unique bifunctional inhibition of the growth of endothelial cells and vascular remodeling. We are now examining the potential synergistic effect of a combinational use of β-HIVS and other clinically-used VEGFR2 inhibitors in the Matrigel plug assay, based upon our previous finding that the combination of β-HIVS and STI571 suppresses phosphorylation of the BCR/ABL-encoded tyrosine kinase more efficiently than either β-HIVS or STI571 alone in K562 cells.[28]

Acknowledgments

The authors thank Dr K. Umezawa (Keio University, Japan), Dr J. K. Yamashita (Kyoto University, Japan), and Dr R. Nishiwaki (Gifu University, Japan) for providing HUVEC, CCE/nLacZ ES cells and the ERK-specific monoclonal antibody, respectively. This study was supported in part by grants from the Foundation for Promotion of Cancer Research in Japan (to S. K.), and the Chemical Genomics Research Project from RIKEN (to S. K.).

References

1 Carmeliet P. Angiogenesis in life, disease and medicine. *Nature* 2005; **438**: 932–6.
2 Mazitschek R, Giannis A. Inhibitors of angiogenesis and cancer-related receptor tyrosine kinases. *Curr Opin Chem Biol* 2004; **8**: 432–41.
3 Bach F, Uddin FJ, Burke D. Angiopoietin in malignancy. *Eur J Surg Oncol* 2007; **33**: 7–15.
4 Jones N, Iljin K, Dumont DJ, Alitalo K. Tie receptors: new modulators of angiogenic and lymphangiogenic responses. *Nat Rev Mol Cell Biol* 2001; **2**: 257–67.
5 Ferrara N, Kerbel R. Angiogenesis as a therapeutic target. *Nature* 2005; **438**: 967–74.
6 Manley PW, Bold G, Bruggen J *et al.* Advances in the structural biology, design and clinical development of VEGF-R kinase inhibitors for the treatment of angiogenesis. *Biochim Biophys Acta* 2004; **1697**: 17–27.
7 Noble ME, Endicott JA, Johnson LN. Protein kinase inhibitors: insights into drug design from structure. *Science* 2004; **303**: 1800–5.
8 Hashimoto S, Xu M, Masuda Y *et al.* β-Hydroxyisovalerylshikonin inhibits the cell growth of various cancer cell lines and induces apoptosis in leukemia HL-60 cells through a mechanism different from those of Fas and etoposide. *J Biochem* 1999; **125**: 17–23.
9 Hashimoto S, Xu Y, Masuda Y *et al.* β-Hydroxyisovalerylshikonin is a novel and potent inhibitor of protein tyrosine kinases. *Jpn J Cancer Res* 2002; **93**: 944–51.
10 Hisa T, Kimura Y, Takada K, Suzuki F, Takigawa M. Shikonin, an ingredient of *Lithospermun erythrorhizon*, inhibits angiogenesis *in vivo* and *in vitro*. *Anticancer Res* 1998; **18**: 783–90.
11 Botella LM, Sanchez-Elsner T, Sanz-Rodriguez F *et al.* Transcriptional activation of *endoglin* and transforming growth factor-β signaling components by cooperative interaction between Sp1 and KLF6: their potential role in the response to vascular injury. *Blood* 2002; **100**: 4001–410.
12 Suzuki Y, Komi Y, Ashino H *et al.* Retinoic acid controls blood vessel formation by modulating endothelial and mural cell interaction via suppression of Tie2 signaling in vascular progenitor cells. *Blood* 2004; **104**: 166–9.
13 Komi Y, Ohno O, Suzuki Y *et al.* Inhibition of tumor angiogenesis by targeting endothelial surface ATP synthase with sangivamycin. *Jpn J Clin Oncol* 2007; **37**: 867–73.
14 Sawano A, Takahashi T, Yamaguchi S, Aonuma M, Shibuya M. Flt-1 but not KDR/Fll-1 tyrosine kinase is a receptor for placenta growth factor, which is related to vascular endothelial growth factor. *Cell Growth Differ* 1996; **7**: 213–21.
15 Hata Y, Duh E, Zhang K, Robinson GS, Aiello LP. Transcription factors Sp1 and Sp3 alter vascular endothelial growth factor receptor expression through a novel recognition sequence. *J Biol Chem* 1998; **273**: 19294–303.
16 Shimada J, Suzuki Y, Kim SJ, Wang PC, Matsumura M, Kojima S. Transactivation via RAR/RXA–Sp1 interaction: characterization of binding between Sp1 and GC box motif. *Mol Endocrinol* 2001; **15**: 1677–92.
17 Dube A, Akbarali Y, Sato TN, Libermann TA, Oettgen P. Role of the Ets transcription factors in the regulation of the vascular-specific Tie2 gene. *Circ Res* 1999; **84**: 1177–85.
18 Lee JA, Suh DC, Kang JE *et al.* Transcriptional activity of Sp1 is regulated by molecular interactions between the zinc finger DNA binding domain and the inhibitory domain with corepressors, and this interaction is modulated by MEK. *J Biol Chem* 2005; **280**: 28061–71.
19 Suzuki Y, Shimada J, Shudo K, Matsumura M, Crippa MP, Kojima S. Physical interaction between retinoic acid receptor and Sp1: mechanism for induction of urokinase by retinoic acid. *Blood* 1999; **93**: 4264–76.

doi: 10.1111/j.1349-7006.2008.01049.x

20 Wilhelm SM, Carter C, Tang L *et al.* BAY 43–9006 exhibits broad spectrum oral antitumor activity and targets the RAF/MEK/ERK pathway and receptor tyrosine kinases involved in tumor progression and angiogenesis. *Cancer Res* 2004; **64**: 7099–109.
21 Merchant JLM, Todisco A. Sp1 phosphorylation by Erk 2 stimulates DNA binding. *Biochem Biophys Res Commun* 1999; **254**: 454–61.
22 Lee S, Chen TT, Barber CL *et al.* Autocrine VEGF signaling is required for vascular homeostasis. *Cell* 2007; **130**: 691–703.
23 Kobayashi H, Lin PC. Angiopoietin/Tie2 signaling, tumor angiogenesis and inflammatory diseases. *Front Biosci* 2005; **10**: 666–74.
24 Verheul HM, Pinedo HM. Possible molecular mechanisms involved in the toxicity of angiogenesis inhibition. *Nat Rev Cancer* 2007; **7**: 475–85.
25 Mori Y, Sahara H, Matsumoto K *et al.* Downregulation of *Tie2* gene by a novel antitumor sulfolipid, 3'-sulfoquinovosyl-1'-monoacylglycerol, targeting angiogenesis. *Cancer Sci* 2008; **99**: 1063–70.
26 De Palma M, Venneri MA, Galli R *et al.* Tie2 identifies a hematopoietic lineage of proangiogenic monocytes required for tumor vessel formation and a mesenchymal population of pericyte progenitors. *Cancer Cell* 2005; **8**: 211–26.
27 Venneri MA, De Palma M, Ponzoni M *et al.* Identification of proangiogenic TIE2-expressing monocytes (TEMs) in human peripheral blood and cancer. *Blood* 2007; **109**: 5276–85.
28 Masuda Y, Nishida A, Hori K *et al.* β-Hydroxyisovalerylshikonin induces apoptosis in human leukemia cells by inhibiting the activity of a polo-like kinase 1 (PLK1). *Oncogene* 2003; **22**: 1012–23.

Supporting Information

Additional Supporting Information may be found in the online version of this article:

Fig. S1. Morphological changes in the vasculature in the kidney, tracheal mucosa and liver.

Fig. S2. Effect of β-HIVS on proteinuria.

Fig. S3. Induction of apotosis in HUVEC cultures by β-HIVS.

Please note: Wiley-Blackwell are not responsible for the content or functionality of any supporting materials supplied by the authors. Any queries (other than missing material) should be directed to the corresponding author for the article.

nature
cell biology

Differential function of Tie2 at cell–cell contacts and cell–substratum contacts regulated by angiopoietin-1

Shigetomo Fukuhara[1,6], Keisuke Sako[1], Takashi Minami[2], Kazuomi Noda[1], Hak Zoo Kim[3], Tatsuhiko Kodama[2], Masabumi Shibuya[4], Nobuyuki Takakura[5], Gou Young Koh[3] and Naoki Mochizuki[1,6]

Tie2 belongs to the receptor tyrosine kinase family and functions as a receptor for Angiopoietin-1 (Ang1). Gene-targeting analyses of either *Ang1* or *Tie2* in mice reveal a critical role of Ang1–Tie2 signalling in developmental vascular formation. It remains elusive how the Tie2 signalling pathway plays distinct roles in both vascular quiescence and angiogenesis. We demonstrate here that Ang1 bridges Tie2 at cell–cell contacts, resulting in *trans*-association of Tie2 in the presence of cell–cell contacts. In clear contrast, in isolated cells, extracellular matrix-bound Ang1 locates Tie2 at cell–substratum contacts. Furthermore, Tie2 activated at cell–cell or cell–substratum contacts leads to preferential activation of Akt and Erk, respectively. Microarray analyses and real-time PCR validation clearly show the differential gene expression profile in vascular endothelial cells upon Ang1 stimulation in the presence or absence of cell–cell contacts, implying downstream signalling is dependent upon the spatial localization of Tie2.

Vascular development is coordinated by endothelial-specific receptor tyrosine kinases and their ligands: vascular endothelial growth factor (VEGF)–VEGF-receptor (VEGFR), ephrin–Eph receptor, and angiopoietin (Ang)–Tie receptor [1]. The Tie1 and Tie2 receptors constitute the Tie receptor family. Gene-targeting analyses have revealed the essentiality of these vascular endothelial receptor tyrosine kinases for vascular formation [1]. Even after the establishment of vascular network, neovessel formation is observed in ischemic diseases and tumours.

Tie2 maintains the vascular integrity of mature vessels by enhancing endothelial barrier function[2–6] and inhibiting apoptosis of endothelial cells[7–9]. Tie2 functions as a receptor for Ang family proteins (Ang1–4). Mice overexpressing Ang1 develop vessels resistant to inflammatory agent-induced leakage[10,11]. Thus, quiescence of blood vessels is thought to be mediated by Ang1–Tie2 signalling. Tie2 signalling is also suggested to promote cell migration and to be involved in VEGF-induced neovascularization and pathological angiogenesis, as opposed to the maintenance of cell quiescence[12–18]. Consistently, Tie2 is not only tyrosine phosphorylated in the endothelium of normal adult tissues, but is also highly expressed in the endothelium of neovessels of regenerating organs and tumours[19,20].

In the quiescent vessels, the endothelial cells tightly contact each other and do not proliferate[19]. On the other hand, during angiogenesis, the cells that lose cell–cell contacts are allowed to proliferate and migrate, thereby resulting in sprouting and branching from the pre-existing vessels to form neovasculature[19]. At present, it is unknown how Tie2 signalling is involved in both vascular quiescence and angiogenesis. Thus, we investigated Ang1–Tie2 signalling in the presence or absence of vascular endothelial cell–cell contacts.

RESULTS

Ang1 induces the translocation of Tie2 at cell–cell contacts

To first elucidate how Tie2 signalling controls vascular quiescence, we examined the localization of Tie2 in confluent human umbilical vein endothelial cells (HUVECs). Tie2 was broadly expressed on the plasma membrane in unstimulated cells. After stimulation with either cartilage oligomeric matrix protein (COMP)–Ang1, a potent Ang1 variant [14], or native Ang1, Tie2 was accumulated at the cell–cell contacts marked by vascular endothelial cadherin (VE-cadherin) (Fig. 1a and Supplementary Information, Fig. S1a). Similar relocation of Tie2 was observed in human arterial endothelial cells (Supplementary Information, Fig. S1b). The relocation of Tie2 was observed within 5 min after the stimulation, becoming more prominent during 15–45 min (Supplementary Information, Fig. S1c). Tie2 was then gradually endocytosed and disappeared from cell–cell contacts. Re-exposure to COMP–Ang1 6 h after the first stimulation re-induced accumulation of Tie2 at cell–cell contacts (Supplementary Information, Fig. S1d–f). These findings indicate that Ang1 induces relocation of Tie2 to cell–cell contacts, which is also supported by time-lapse imaging of cells expressing Tie2 carboxy-terminally

[1]Department of Structural Analysis, National Cardiovascular Center Research Institute, 5-7-1 Fujishirodai, Suita, Osaka 565-8565, Japan. [2]The Research Center for Advanced Science and Technology, University of Tokyo, Laboratory for System Biology and Medicine, 4-6-1, Komaba, Meguro, Tokyo, 153-8904, Japan. [3]Biomedical Research Center and Department of Biological Sciences, Korea Advanced Institute of Science and Technology, Guseong-dong, Daejeon, 305-701, Korea. [4]Division of Genetics, Institute of Medical Science, University of Tokyo, 4-6-1 Shirokane-dai, Minato-ku, Tokyo 108-8639, Japan. [5]Department of Signal Transduction, Research Institute of Microbial Diseases, Osaka University, 3-1 Yamada-oka, Suita, Osaka, 565-0871, Japan.
[6]Correspondence should be addressed to S.F. or N.M. (e-mails: fuku@ri.ncvc.go.jp; nmochizu@ri.ncvc.go.jp)

Received 3 December 2007; accepted 29 February 2008; published online 20 April 2008; DOI: 10.1038/ncb1714

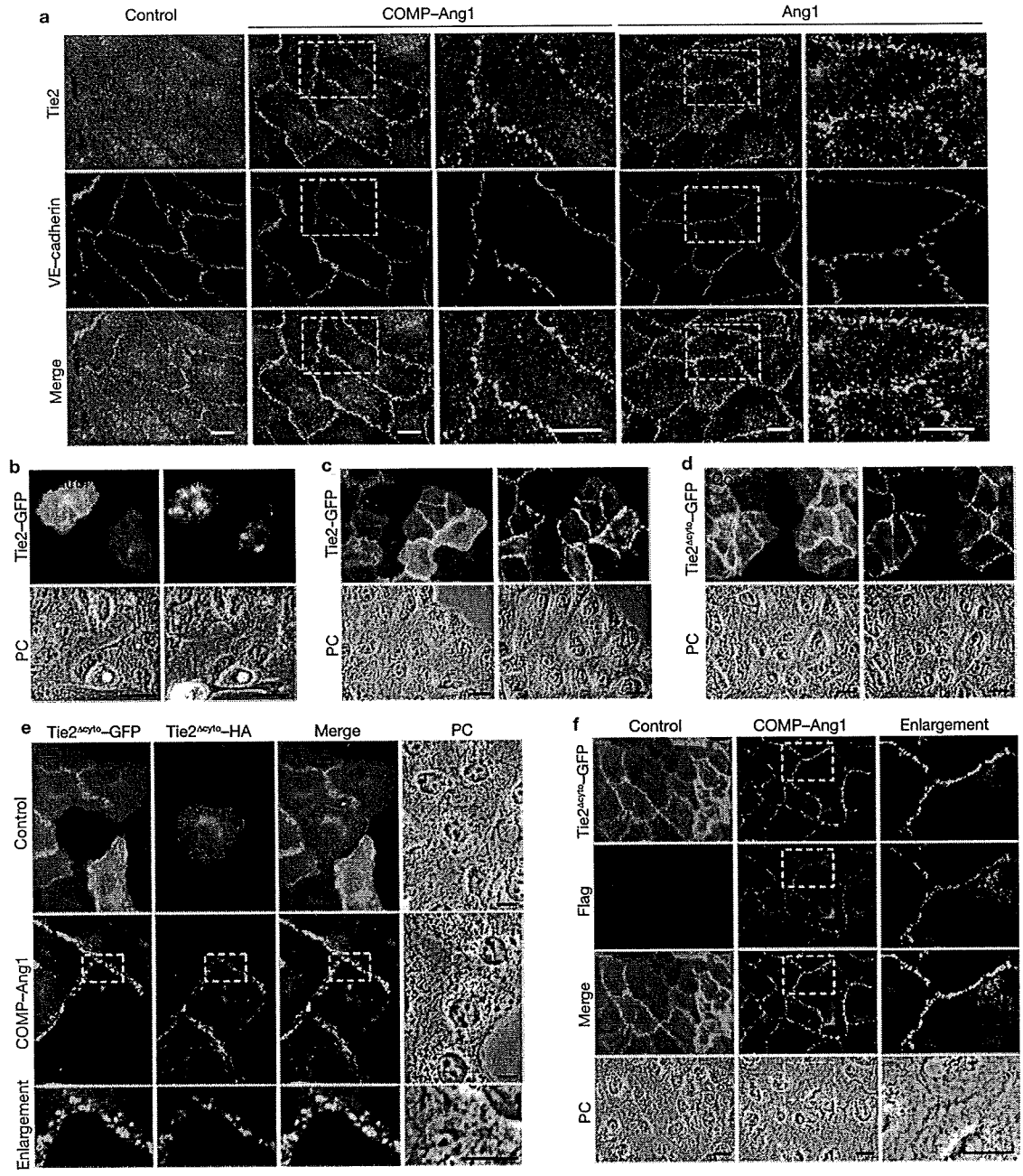

Figure 1 Tie2 is recruited to cell–cell contacts upon Ang1 stimulation in vascular endothelial cells. **(a)** Confluent HUVECs plated on a collagen-coated dish (cells were plated on a collagen-coated dish for the following experiments unless otherwise indicated) were starved in medium 199 containing 0.5% BSA for 3 h and stimulated with vehicle (control), 200 ng ml^{-1} COMP–Ang1, or 600 ng ml^{-1} Ang1 for 20 min (COMP–Ang1 and native Ang1 were used at these concentrations throughout the following experiments unless otherwise indicated). After stimulation, the cells were fixed, immunostained with anti-Tie2 (top) and anti-VE-cadherin (middle) antibodies. Fluorescence images were obtained using an Olympus IX-81 inverted microscope. The boxed areas are enlarged on the right. **(b)** CHO cells transfected with the plasmid expressing Tie2–GFP were starved for 3 h and stimulated with COMP–Ang1. Tie2–GFP (top) and phase-contrast (PC, bottom) images of the Tie2–GFP-expressing cells surrounded by those that do not express Tie2–GFP were time-lapse imaged and analysed by MetaMorph 6.1 software. The images before (left) and 1 h after (right) stimulation are shown. **(c)** Tie2–GFP-expressing cells contacting each other were stimulated with COMP–Ang1 and time-lapse imaged. **(d)** CHO cells transfected with the plasmid expressing Tie2Δcyto–GFP were stimulated with COMP–Ang1 and time-lapse imaged. **(e)** CHO cells were transfected with either the plasmid expressing Tie2Δcyto–GFP or that expressing Tie2Δcyto–HA. The next day, the cells expressing Tie2Δcyto–GFP and those expressing Tie2Δcyto–HA were co-plated and stimulated with either vehicle (control) or COMP–Ang1 for 1 h. After stimulation, the cells were stained with anti-HA antibody. GFP (green), HA (red), the merged images, and the phase-contrast images (PC) are shown. The boxed areas are enlarged at the bottom of each image. **(f)** CHO cells transfected with the vector encoding Tie2Δcyto–GFP were stimulated as described in **e**. To visualize Flag-tagged COMP–Ang1, the stimulated cells were stained with anti-Flag antibody. GFP (green), Flag (red), the merged images (merge), and the phase-contrast images (PC) are shown as labelled on the left. The boxed areas are enlarged in the right panels. The scale bars represent 20 μm (**a**, **b**, **c**, **d**, **f**), and 10 μm (**e**), respectively.

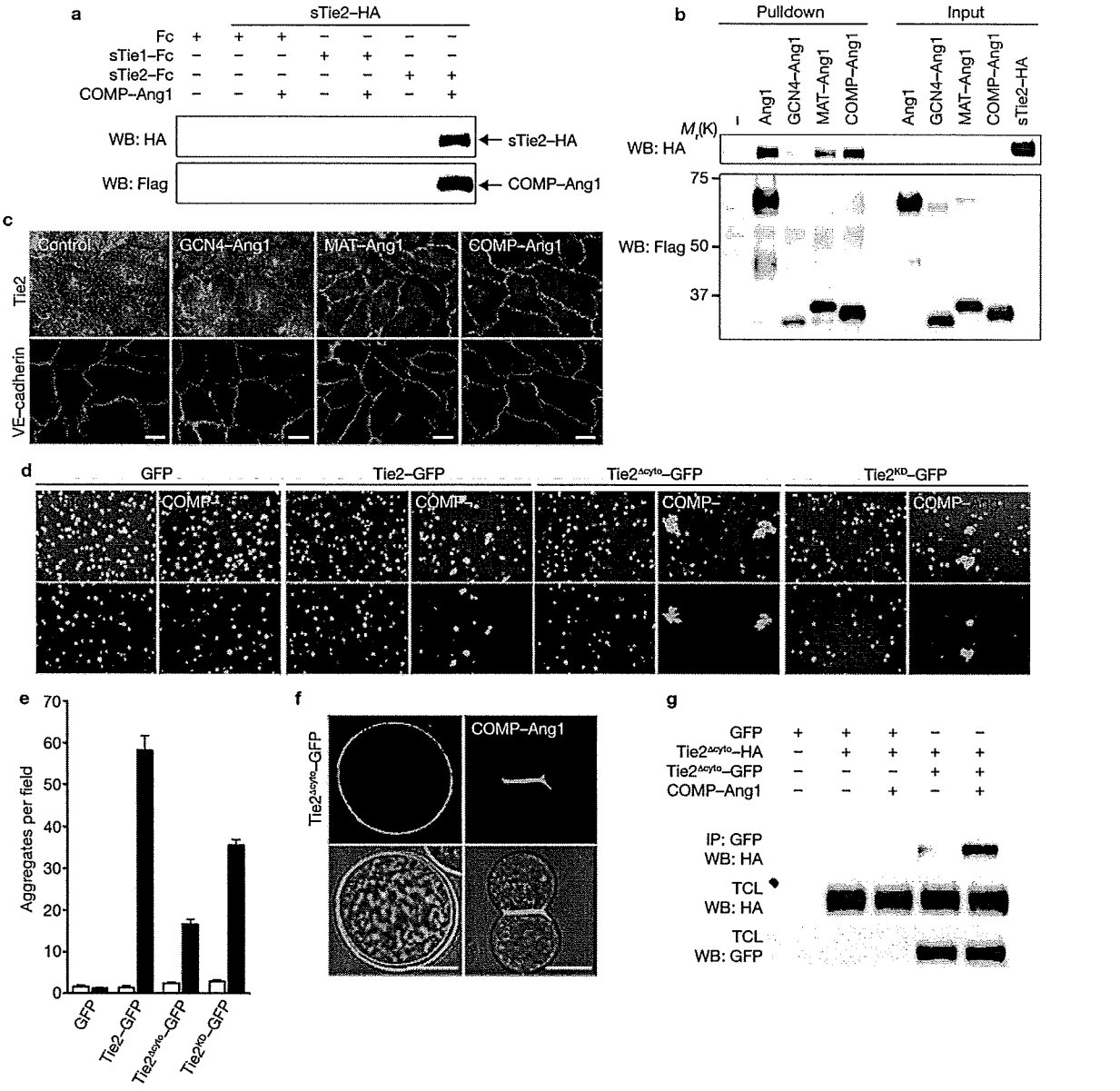

Figure 2 Ang1 induces *trans*-association of Tie2 at cell–cell contacts. **(a)** *In vitro* binding of sTie2–HA to sTie1–Fc or sTie2–Fc. Binding in the presence or absence of COMP–Ang1 was examined as described in Methods. Arrows indicate co-precipitated sTie2–HA and COMP–Ang1 proteins. **(b)** The association of sTie2–HA to sTie2–Fc by Ang1, GCN4–Ang1, MAT–Ang1, or COMP–Ang1 was similarly examined as in **a**. **(c)** Confluent HUVECs were stimulated with vehicle (control), 200 ng ml^{-1} GCN4–Ang1, MAT–Ang1 or COMP–Ang1 for 20 min, and stained with anti-Tie2 (upper panels) and anti-VE-cadherin (lower panels) antibodies. The scale bars represent 20 μm. **(d)** Aggregation of 293F cells in suspension expressing GFP, Tie2–GFP, Tie2Δcyto–GFP and Tie2KD–GFP was induced by vehicle (control; left of each panel) and COMP–Ang1 (right of each panel), as described in Methods. Upper and lower images of each panel show the phase-contrast and GFP images. **(e)** To quantify the cell aggregation observed in **d**, the number of cell aggregates per field of view was counted. An aggregate was defined as cell mass consisting of more than 4 cells. The number of aggregates for cells stimulated with vehicle and COMP–Ang1 is shown as white and black columns, respectively. Data are expressed as mean number ± s.d. of, at least, 10 different fields. **(f)** 293F cells expressing Tie2Δcyto–GFP were incubated with vehicle (control; left column) and COMP–Ang1 (right column). Upper and lower panels show the confocal GFP images merged without or with the DIC images, respectively. The scale bars represent 10 μm. **(g)** 293F cells expressing Tie2Δcyto–HA were suspended with either those expressing Tie2Δcyto–GFP or those expressing GFP, and stimulated with 400 ng ml^{-1} of COMP–Ang1 for 1 h. Cell lysates were immunoprecipitated with anti-GFP antibody. Immunoprecipitates (IP) and aliquots of cell lysate (TCL) were subjected to Western blot analysis (WB) with anti-HA and anti-GFP antibodies. Uncropped images of **a**, **b**, and **g** are shown in Supplementary Information, Fig. S8.

fused with green fluorescent protein (GFP) (Tie2–GFP) (Supplementary Information, Fig. S1g, h and Movie 1).

VEGFR2 is known to associate with VE-cadherin at cell–cell contacts[21,22]. Thus, we assumed that VE-cadherin might be involved in Tie2 relocation to cell–cell contacts. However, Tie2 relocation at cell–cell contacts was still observed in VE-cadherin–depleted HUVECs, while β-catenin disappeared from cell–cell contacts (Supplementary Information, Fig. S2a, c). Tie2 staining at cell–cell contacts was slightly

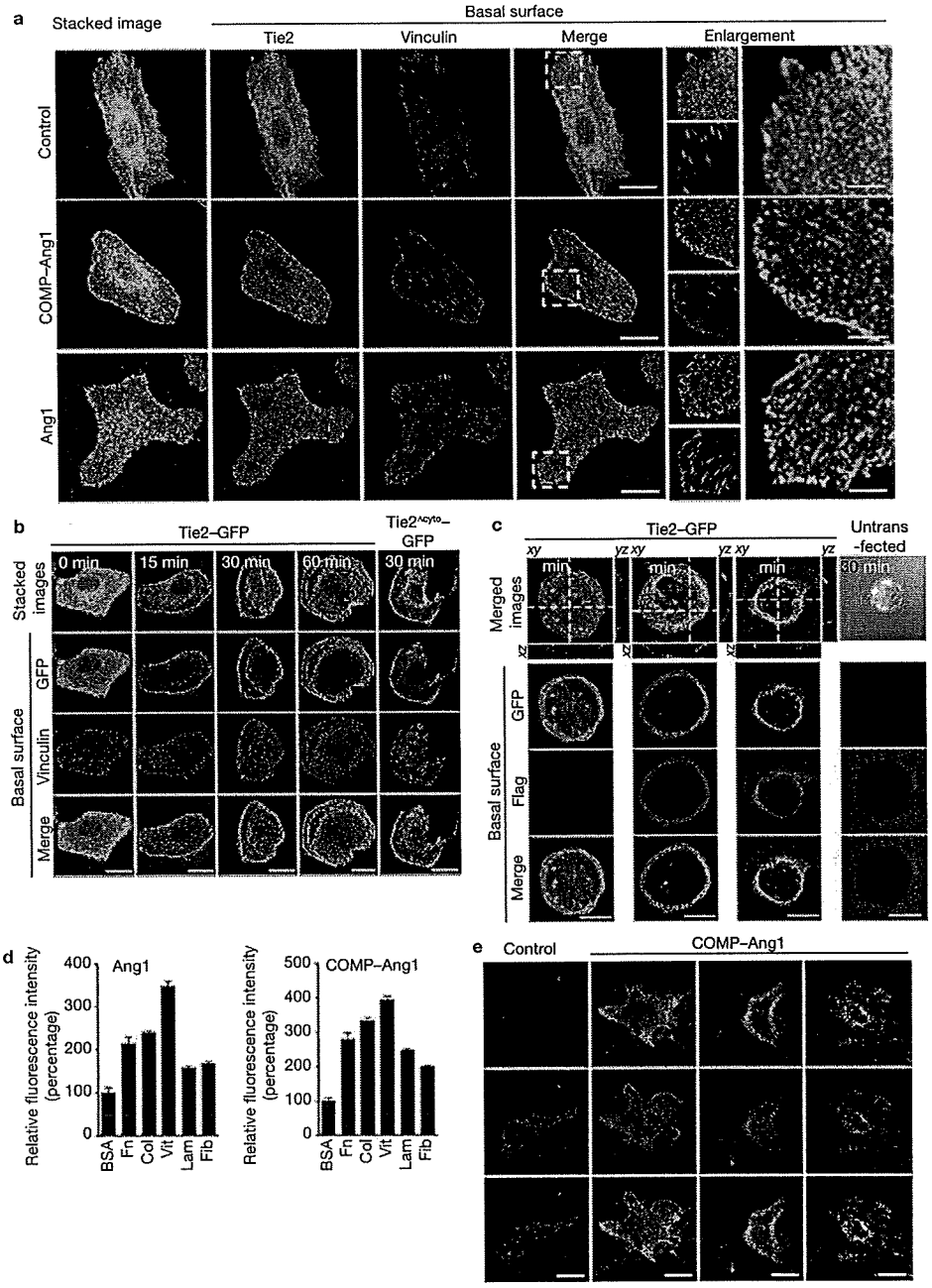

Figure 3 ECM-bound Ang1 anchors Tie2 to cell–substratum contacts in the absence of cell–cell adhesions. (**a**) Sparse HUVECs were stimulated with vehicle (control), COMP–Ang1 or Ang1, and then immunostained with anti-Tie2 and anti-vinculin antibodies. Images were obtained using a confocal microscope. Stacked *xy* images (left), Tie2 (green), vinculin (red) and merged (merge) images of the cell–substratum interface (basal surface) are shown. The boxed areas in the merged images are enlarged (right panels). (**b**) Time course (for the time indicated) of localization of Tie2–GFP and vinculin in CHO cells expressing Tie2–GFP was examined similarly to a. Localization of Tie2Δcyto–GFP after stimulation for 30 min was also examined (left column). (**c**) Localization of COMP–Ang1 (Flag, red) and Tie2–GFP (green) after stimulation with COMP–Ang1 in CHO cells expressing Tie2–GFP was examined similarly to **a**. Untransfected CHO cells were also stimulated with COMP–Ang1, and immunostained with anti-Flag antibody (right column). A DIC image (top) is displayed at the top. (**d**) Binding of Ang1 and COMP–Ang1 to ECM was examined by immunofluorescence analysis as described in Supplementary Methods. Glass-base dishes were coated with BSA (BSA), fibronectin (Fn), collagen (Col), vitronectin (Vit), laminin (Lam), and fibrinogen (Fib), and incubated with Ang1 (left panel) or COMP–Ang1 (right panel). ECM-bound Ang1 and COMP–Ang1 were detected by staining with anti-Flag antibody. Relative immunofluorescence intensity was expressed as a percentage of that detected in a BSA-coated dish. Data are expressed as mean ± s.d. of the fluorescence intensity of 6 different fields. (**e**) Sparse HUVECs expressing both Tie2–GFP and RFP–Crk and those expressing Tie2–GFP were stimulated with COMP–Ang1 or vehicle (control). After stimulation for 20 min, the cells were washed and treated with cytoskeleton stabilizing buffer as described in Methods. The cells expressing Tie2–GFP were immunostained with either anti-vinculin or anti-Flag antibody. GFP (Tie2–GFP), and RFP (RFP–Crk) or Alexa 546 (vinculin or COMP–Ang1) confocal images of the cell–substratum interface, and merged images (bottom) are shown. The scale bars in merged (**a**, **b**, **c**, and **e**) and enlarged images (**a**) represent 20 μm and 5 μm, respectively.

diminished compared to the control cells. Consistently, we found that Tie2 did not co-immunoprecipitate with VE-cadherin in the COMP-Ang1-stimulated HUVECs, although VEGFR2 co-immunoprecipitated with VE-cadherin in those stimulated by VEGF (Supplementary Information, Fig. S2d, e). Furthermore, depletion of platelet and endothelial cell adhesion molecule-1 (PECAM-1) did not affect the relocation of Tie2 to cell–cell contacts (Supplementary Information, Fig. S2b, c). These results indicate that VE-cadherin and PECAM-1 are not essential for Tie2 localization at cell–cell contacts, although cell adhesions by these molecules may affect the localization of Tie2 by stabilizing cell–cell contacts.

We hypothesized that the interaction of Tie2 expressed in adjoining cells might be required for the accumulation of Tie2 at cell–cell contacts. We employed Chinese hamster ovary (CHO) cells that do not express endogenous Tie2 and CHO cells expressing Tie2–GFP. By monitoring Tie2–GFP upon COMP–Ang1 stimulation, we could distinguish the dynamics of Tie2–GFP in the presence or absence of Tie2 expression between adjoining CHO cells. Tie2–GFP was internalized upon stimulation with COMP–Ang1 when a Tie2–GFP-expressing cell was surrounded by wild-type CHO cells (Fig. 1b and Supplementary Information, Movie2). In contrast, COMP–Ang1 stimulation induced Tie2–GFP translocation to the cell–cell borders between adjacent cells expressing Tie2–GFP, although Tie2–GFP was homogeneously expressed on the plasma membrane before the stimulation (Fig. 1c and Supplementary Information, Fig. S2f and Movie3). Notably, Tie2–GFP lacking the cytoplasmic domain of Tie2 (Tie2Δcyto–GFP) relocated to the borders between adjacent cells expressing Tie2Δcyto–GFP (Fig. 1d and Supplementary Information, Movie 4). To further test the effect of the extracellular domain of Tie2 between adjoining cells on the accumulation of Tie2 at cell–cell contacts, CHO cells expressing Tie2Δcyto–GFP and those expressing Tie2Δcyto–HA (a mutant Tie2 lacking the cytoplasmic domain tagged with HA) were co-plated and stimulated with COMP–Ang1. In the unstimulated cells, both Tie2Δcyto–GFP and Tie2Δcyto–HA were broadly expressed on the plasma membrane without any colocalization. Once stimulated with COMP–Ang1, Tie2Δcyto–GFP and Tie2Δcyto–HA colocalized at the cell–cell borders between cells expressing Tie2Δcyto–GFP and cells expressing Tie2Δcyto–HA (Fig. 1e). Interestingly, COMP–Ang1 was also detected at the cell–cell borders where Tie2Δcyto–GFP localized (Fig. 1f). Collectively, these findings suggest that Ang1 induces *trans*-association of Tie2 at cell–cell contacts independently of its intracellular signalling.

Internalization was further analysed by a confocal microscope. In Tie2–GFP-expressing CHO cells surrounded by wild-type CHO cells, Tie2–GFP was clearly internalized upon COMP–Ang1 stimulation, while in either Tie2Δcyto–GFP-expressing CHO cells or kinase-negative Tie2–GFP (Tie2KD–GFP)-expressing CHO cells, Tie2 was not internalized (Supplementary Information, Fig. S2g). These data indicate that endocytosis of Tie2 is triggered by its intracellular signalling, and suggest that Ang1-induced localization of Tie2 at cell–cell contacts depends upon the balance between *trans*-association of activated Tie2 and the internalization of Tie2.

Trans-association of Tie2 induced by oligomerized Ang1

To explore whether the *trans*-association of Tie2 is provoked by oligomerized Ang1, we first biochemically analysed the association of Tie2 using recombinant Tie proteins. We tested the association of immunoglobulin Fc-domain tagged extracellular domain of either Tie1 or Tie2 with the HA-tagged extracellular domain of Tie2, as explained in Supplementary Fig. 3a and 3b. HA-tagged Tie2 bound to sTie2–Fc but not sTie1–Fc in the presence of COMP–Ang1 (Fig. 2a). We then tested the association of sTie2–HA with sTie2–Fc in the presence of various forms of Ang1 (GCN4–Ang1, dimer; native Ang1 and MAT–Ang1, tetramer; COMP–Ang1, pentamer)[14]. The association of sTie2–HA with sTie2–Fc was induced by native Ang1, MAT–Ang1, and COMP–Ang1, which can form multimers of Ang1, but not by GCN4–Ang1 (Fig. 2b). Consistently, multimerized Ang1 induced the relocation of Tie2 at cell–cell contacts (Fig. 2c).

We further tested the possibility of Ang1-mediated bridging of Tie2 by using 293 cells in suspension (293F). Tie2–GFP-expressing 293F cells but not GFP-expressing 293F cells aggregated upon COMP–Ang1 and native Ang1 stimulation (Fig. 2d, e and Supplementary Information, Fig. S3c, d). The number of aggregates in Tie2–GFP-expressing cells increased more than in Tie2Δcyto–GFP-expressing cells and Tie2KD–GFP-expressing cells that were resistant to internalization of Tie2 (Fig. 2e and Supplementary Information, Fig. S2g). In contrast, the size of the aggregates was increased in Tie2Δcyto–GFP-expressing cells and Tie2KD–GFP-expressing cells compared to Tie2–GFP-expressing cells (Supplementary Information, Fig. S3e), suggesting that intracellular signalling may affect Ang1-mediated Tie2 *trans*-association probably through Tie2 internalization.

In the aggregated cells, Tie2Δcyto–GFP clearly localized at the sites of cell–cell contacts (Fig. 2f). Similar localization of Tie2Δcyto–GFP at cell–cell contacts was observed in a murine pro-B cell line, BaF3 cells, stably expressing Tie2Δcyto–GFP (BaF–Tie2ΔcytoGFP) upon COMP–Ang1 stimulation (Supplementary Information, Fig. S3h). VEGF did not induce aggregation of 293F cells expressing VEGFR2, although VEGFR2 is reported to localize to cell–cell contacts [21,23](Supplementary Information, Fig. S3f, g). When 293F cells expressing Tie2Δcyto–GFP and those expressing Tie2Δcyto–HA were co-cultured in suspension and stimulated with COMP–Ang1, both Tie2 were co-immunoprecipitated (Fig. 2g). Furthermore, when BaF–Tie2ΔcytoGFP cells and BaF3 cells stably expressing Tie2Δcyto–HA (BaF–Tie2ΔcytoHA) were mixed and stimulated with COMP–Ang1 in suspension, both truncated forms of Tie2 were also co-immunoprecipitated (Supplementary Information, Fig. S3i). These results together with biochemical data and the co-localization of Tie2 lacking its cytoplasmic domain (Fig. 1e) indicate the *trans*-association of Tie2 occurs at cell–cell contacts upon oligomerized Ang1 stimulation.

Tie2 localizes to cell–substratum contacts in the absence of cell–cell contacts

We next examined Ang1-induced localization of Tie2 in sparse HUVECs. In subconfluent HUVECs, Tie2 was preferentially recruited to cell–cell contacts upon COMP–Ang1 stimulation (Supplementary Information, Fig. S4a). However, when stimulated in the absence of cell–cell contacts, Tie2 localized to the periphery of the extended membrane that was close to but different from vinculin- and paxillin-positive focal complexes (FCs) (Fig. 3a and Supplementary Information, Fig. S4b). We further investigated COMP–Ang1-induced localization of Tie2–GFP in CHO cells. Tie2–GFP was localized to the periphery at 15, 30 and 60 min after stimulation. We noticed additional GFP-positive lines at cell–substratum contacts in the cells stimulated for 30 min and 60 min, reflecting the footprints of membrane extension during cell movement (Fig. 3b).

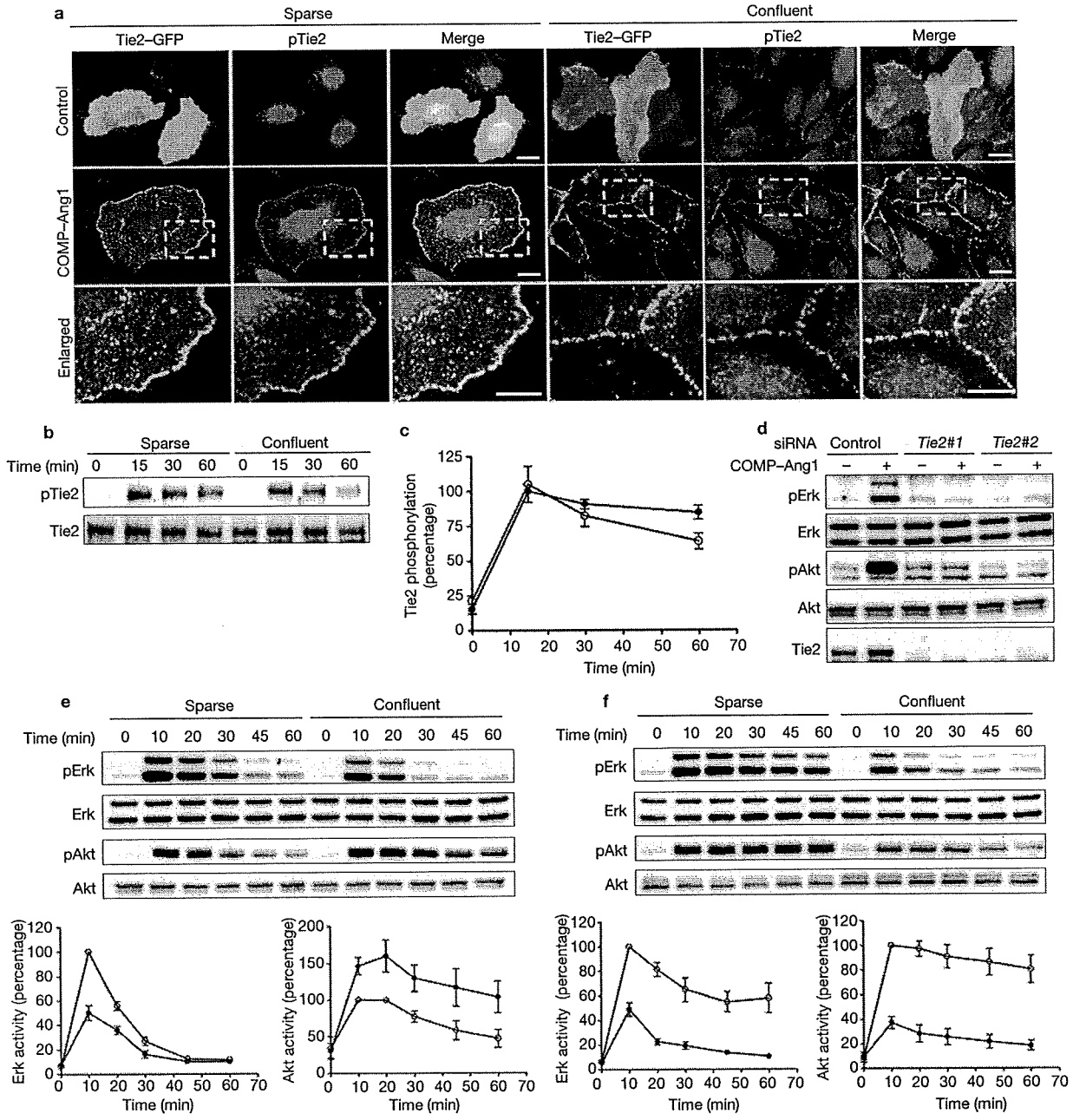

Figure 4 *Trans*-association of Tie2 leads to the preferential activation of Akt. (**a**) Sparse and confluent HUVECs were transfected with the plasmid encoding Tie2–GFP, stimulated with either vehicle (control) or COMP–Ang1, and immunostained with an anti-phospho Tie2 (pTie2) antibody. Images of Tie2–GFP (green), pTie2 (red), and the merged images (merge) are shown. The boxed areas in the panels are enlarged at the bottom of each image. The scale bars in the merged and the enlarged images represent 20 and 5 μm, respectively. (**b**) Sparse and confluent HUVECs were starved and stimulated with COMP–Ang1 for the time (min) indicated at the top. Cell lysates were immunoprecipitated with anti-Tie2 antibody. Immunoprecipitates and aliquots of cell lysate were subjected to western blot analysis with anti-phosphotyrosine (pTie2) and anti-Tie2 (Tie2) antibodies. (**c**) Phosphorylated Tie2 observed in **b** was quantified. Tie2 phosphorylation represents the ratio of phosphorylated Tie2 to total Tie2 as a percentage of the ratio in the sparse cells stimulated for 15 min. Values are expressed as means ± s.d. from five independent experiments. (**d**) HUVECs transfected with control siRNA (control) or with two independent siRNAs targeting different sequences of *Tie2* (Tie2 No.1 and Tie2 No.2) were starved and stimulated with vehicle (–) and COMP–Ang1 (+) for 15 min. Cell lysates were subjected to immunoblot analysis for analysing Erk and Akt phosphorylation. (**e**) Sparse and confluent HUVECs were stimulated with COMP–Ang1 for the time (min) indicated at the top. Activation of Erk and Akt was analysed. Graphs at the bottom left and right panels show time course of Erk and Akt activation of the sparse cells (open circle) and the confluent cells (filled circle) in response to COMP–Ang1. Erk or Akt activity represents the ratio of phospho-Erk or phospho-Akt to total Erk or total Akt as a percentage of the ratio observed in sparse cells stimulated for 10 min, respectively. Values are expressed as means ± s.d. from five independent experiments. (**f**) Sparse (open circle) and confluent (filled circle) HUVECs were stimulated with growth media and analysed. Uncropped images of **b**, **d**, **e**, **f** are shown in Supplementary Information, Fig. S8.

Likewise, in Tie2Δcyto–GFP-expressing CHO cells, Tie2Δcyto–GFP was found at cell–substratum contacts, indicating the requirement of the extracellular domain of Tie2 for this localization. These Tie2–GFP positive structures at cell–substratum contacts were located close to, but apparently different from, vinculin-marked FCs or focal adhesions (FAs) (Supplementary Information, Fig. S4c). To identify the cell matrix junctions where Tie2 localizes, we carefully compared Tie2–GFP with those of various markers for FCs and FAs in HUVECs plated on fibronectin- and collagen-coated dishes after COMP–Ang1 stimulation. Tie2–GFP at cell–substratum contacts colocalized with none of these markers including vinculin, paxillin, VASP, and talin (Supplementary Information, Fig. S5a–g). Collectively, these results indicate that upon stimulation with Ang1, Tie2 is recruited to the cell periphery and anchored to substratum contacts that are different from FCs and FAs. This is further supported by time-lapse imaging using HUVECs expressing Tie2–GFP and CHO cells expressing either Tie2–GFP or Tie2Δcyto–GFP upon COMP–Ang1 stimulation (Supplementary Information, Movie 6 and 7).

$\alpha_5\beta_1$ integrin associates with fibronectin fibrils to form distinct adhesive structures from FCs and FAs, namely fibrillar adhesions (FBs) where fibrinogenesis occurs[24,25]. Since Cascone *et al.* has reported that Tie2 constitutively associates with $\alpha_5\beta_1$ integrin that binds to fibronectin[26], we examined whether Tie2 localizes at FBs. When Tie2–GFP– or HA-tagged Tie2 (Tie2–HA)–expressing HUVECs plated on a fibronectin-coated dish were stimulated with COMP–Ang1, Tie2 did not colocalize with FB markers (α_5 integrin, assembled fibronectin fibrils and exogenously expressed GFP–tensin) (Supplementary Information, Fig. S5h–j). In addition, depletion of α_5 integrin by siRNA did not affect COMP–Ang1-induced Tie2 localization at cell–substratum contacts (Supplementary Information, Fig. S6a–d). Depletion of another integrin, $\alpha_v\beta_3$, did not alter COMP–Ang1-induced relocation of Tie2 to peripheral cell–substratum contacts (Supplementary Information, Fig. S6 a–c).

We assumed that Ang1 might anchor Tie2 to extracellular matrix (ECM). When Tie2–GFP-expressing CHO cells were sparsely cultured on collagen-coated dishes and stimulated with COMP–Ang1, Tie2–GFP and FLAG-tagged COMP–Ang1 were clearly colocalized at the periphery and bottom of the cells at 5 min after stimulation, with the appearace of a ring (Fig. 3c). After 30 min, we noticed that Ang1 was detected not only with Tie2–GFP but also on the dish surface where the cell was not present (Fig. 3c and Supplementary Information, Fig. S6e), suggesting that Ang1 can bind to ECM. Indeed, Ang1 and COMP–Ang1, but not control protein, could bind to fibronectin, collagen, and vitronectin with high affinity, and bind weakly to laminin and fibrinogen as demonstrated by an ECM–Ang1 binding assay (Fig. 3d and Supplementary Information, Fig. S6f). Adhesive structures formed at cell–substratum contacts such as FCs and FAs are resistant to detergent (0.5% Triton-X100)[27,28]. Whereas Tie2–GFP but not RFP–Crk disappeared upon detergent addition without pretreatment of COMP–Ang1, pretreatment of COMP–Ang1 preserved Tie2–GFP at the bottom of cells as well as RFP–Crk and vinculin (Fig. 3e). These results suggest that Tie2 is anchored by ECM-bound Ang1 to cell–substratum contacts to form novel detergent-resistant adhesive structures, which are different from FCs, FAs and FBs.

Preferential activation of Erk and Akt in the absence and presence of cell–cell contacts upon Ang1 stimulation

We investigated the biological significance of *trans*-associated Tie2 at cell–cell contacts and cell–substratum contact-anchored Tie2 upon Ang1 stimulation. Tie2 under both conditions was phosphorylated at either cell–cell contacts or cell–substratum contacts (Fig. 4a). The extent of Tie2 phosphorylation in HUVECs by COMP–Ang1 did not depend upon the presence of cell–cell contacts (Fig. 4b, c).

Among Tie2-mediated signalling factors[4,19], Akt and Erk are suggested to be important for cell survival, and cell migration and proliferation, respectively[9,29,16,30,31]. We therefore checked the requirement of Tie2 in Ang1-induced Erk and Akt activation in HUVECs, because Ang1 is known to mediate some biological functions through integrins [32,33]. Ang1-dependent phosphorylation of both Erk and Akt in confluent and sparse HUVECs was abolished by depletion of Tie2 (Fig. 4d and data not shown). Under either sparse or confluent culture conditions, COMP–Ang1 induced Erk phosphorylation, which peaked at 10 min after stimulation and declined to the basal level by 45 min (Fig. 4e). However, the maximum level of Erk phosphorylation in the confluent cells was reduced to approximately 50% of that in the sparse cells (Fig. 4e). In clear contrast, the maximum increase in Akt phosphorylation was significantly higher in the confluent cells than in the sparse cells (Fig. 4e), indicating that endothelial cell–cell adhesions positively regulate the Tie2-mediated Akt pathway. We noticed that this preferential activation of Akt was a Tie2-specific signal in the confluent cell culture, because both Erk and Akt activation was suppressed when the endothelial cells were stimulated with growth media in the presence of cell–cell contacts (Fig. 4f).

Activation of Erk by Tie2 at cell–substratum contacts is partly dependent upon focal adhesion kinase and involved in endothelial cell migration

To further explore how Tie2-mediated signalling in isolated cells is influenced by its targeting to cell–substratum contacts, HUVECs were stimulated with COMP–Ang1 under either suspended or substratum-attached conditions. While Tie2 phosphorylation and subsequent Akt activation were comparable between these conditions, Erk activation was higher in substratum-attached cells (Fig. 5a). Similar results were obtained using BaF3 cells stably expressing Tie2 (BaF–Tie2) (Supplementary Information, Fig. S7a–c). These findings suggest that Erk activation by Ang1–Tie2 requires the contacts between cells and substratum, as previously reported for other receptor tyrosine kinases[34,35].

We hypothesized that Ang1–Tie2 at cell–substratum contacts cooperatively function with integrin signalling complexes to induce Erk activation, although Tie2 localized to cell–substratum contacts besides FCs, FAs and FBs. To test this possibility, we examined whether ECM-anchored Ang1 induces Tie2 signalling and modulates integrin adhesions. In HUVECs adhering to a collagen-coated dish, Tie2 diffusely localized at bottom surface of the cells. In clear contrast, Tie2 was found to be punctate and phosphorylated at cell–substratum contacts when the cells were attached to a collagen- and COMP–Ang1-coated dish (Supplementary Information, Fig. S7d, e), indicating the capability of ECM-anchored Ang1 to stimulate Tie2. HUVECs adhering to collagen- and COMP–Ang1-coated substratum exhibited enhanced vinculin accumulation at the most peripheral region of the cells, compared with the cells attached to collagen, as analysed by line-scanning of immunofluorescence intensity (Fig. 5b, c). Consistently, fewer stress fibres and more lamellipodia were observed in the presence of COMP–Ang1 (Supplementary Information, Fig. S7f). These data reveal that Ang1–Tie2 signalling at cell–substratum contacts induces FC formation.

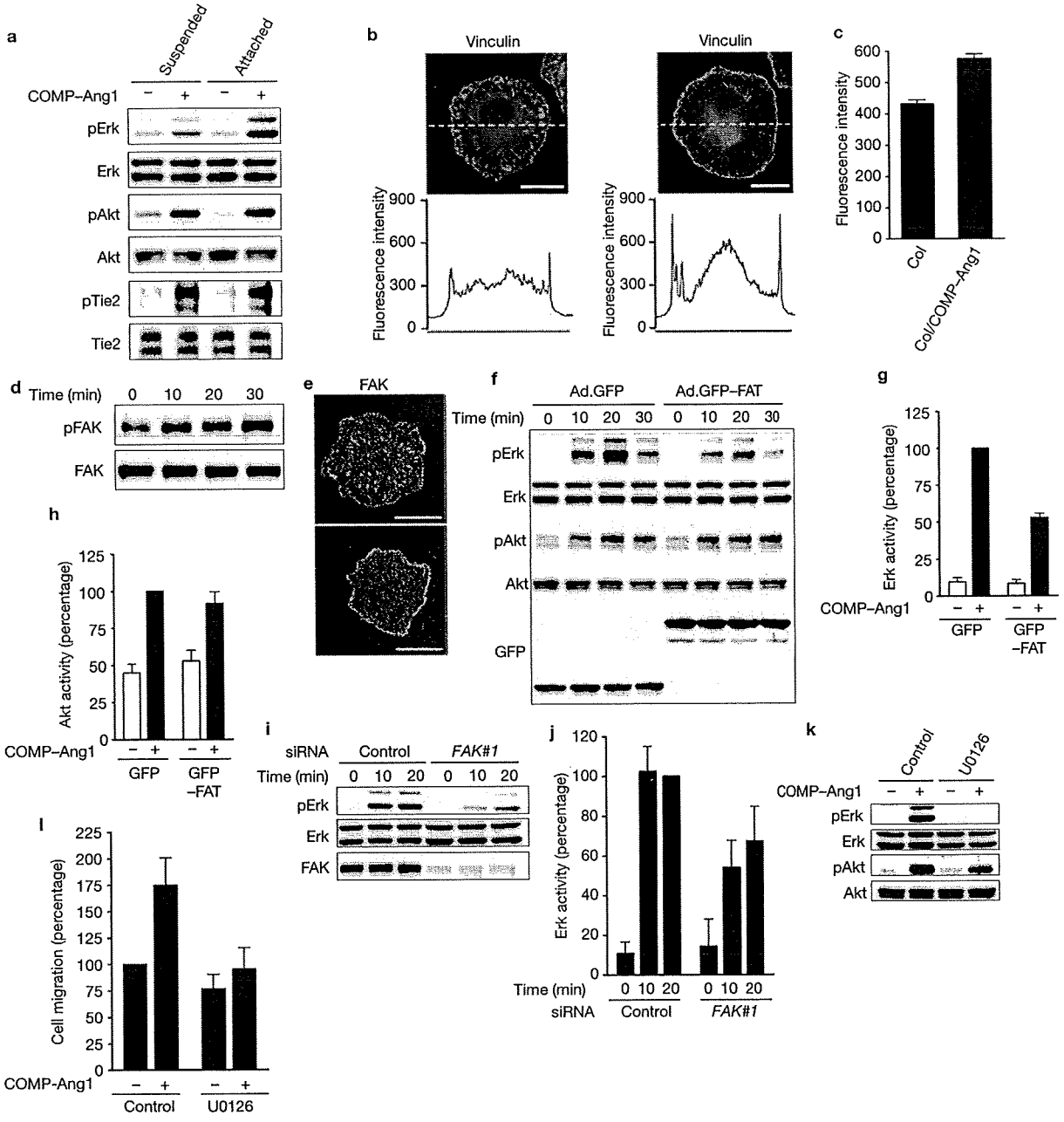

Figure 5 Activation of Erk by Tie2 at cell–substratum contacts partly depends upon FAK and is involved in endothelial cell migration. (**a**) Suspended HUVECs and cells adhered on a as described in Supplementary Methods. (**b**) HUVECs were placed on the COMP–Ang1–unbound collagen-coated dish (Col) or COMP–Ang1–bound collagen-coated dish (Col and COMP–Ang1) for 30 min, and immunostained with anti-vinculin antibody. Focal complexes were analysed by line intensity scan using MetaMorph 6.1 software (fluorescence intensity along the dotted line indicated, bottom panels). (**c**) Quantification of the Results of **b**. Values are expressed as means ± s.d. of fluorescence intensity relative to vinculin at the cell periphery (Col, $n = 60$; Col & COMP–Ang1, $n = 66$). (**d**) Sparse HUVECs starved for 6 h were stimulated with COMP–Ang1 for different times (min). Immunoprecipitates and cell lysate were subjected to western blot analysis with anti-phosphotyrosine (pFAK) and anti-FAK (FAK) antibodies, respectively. (**e**) Localization of FAK was examined similarly to **b**. (**f**) Sparse HUVECs plated on a collagen-coated dish were infected with adenovirus vector encoding either GFP or GFP–FAT as described in Supplementary Information, Methods. Cells stimulated with COMP–Ang1 for 20 min were analysed for Erk and Akt activation. (**g**, **h**) Phosphorylation of Erk (**g**) and Akt (**h**) in **f** was quantified. Values are expressed as means ± s.d. from five independent experiments. (**i**) Effect of knockdown of FAK on Erk activation was examined in control siRNA (control) or *FAK* siRNA-treated HUVECs (FAK No.1). (**j**) Quantification of the results of **i**. Values are expressed as means ± s.d. from 6 independent experiments. (**k**, **l**) MEK–Erk inhibition results in decreased migration of sparse HUVECs stimulated with COMP–Ang1. 20 μM U0126 (a MEK inhibitor) inhibits COMP–Ang1-induced Erk, but not Akt activation (**k**). Migration of HUVECs was analysed as described in Supplementary Methods (**l**). Values are expressed as the mean ± s.d. from 5 independent experiments. The scale bars represent 20 μm (**b**, **e**). Uncropped images of **a**, **d**, **f**, **i**, **k** are shown in Supplementary Information, Fig. S8.

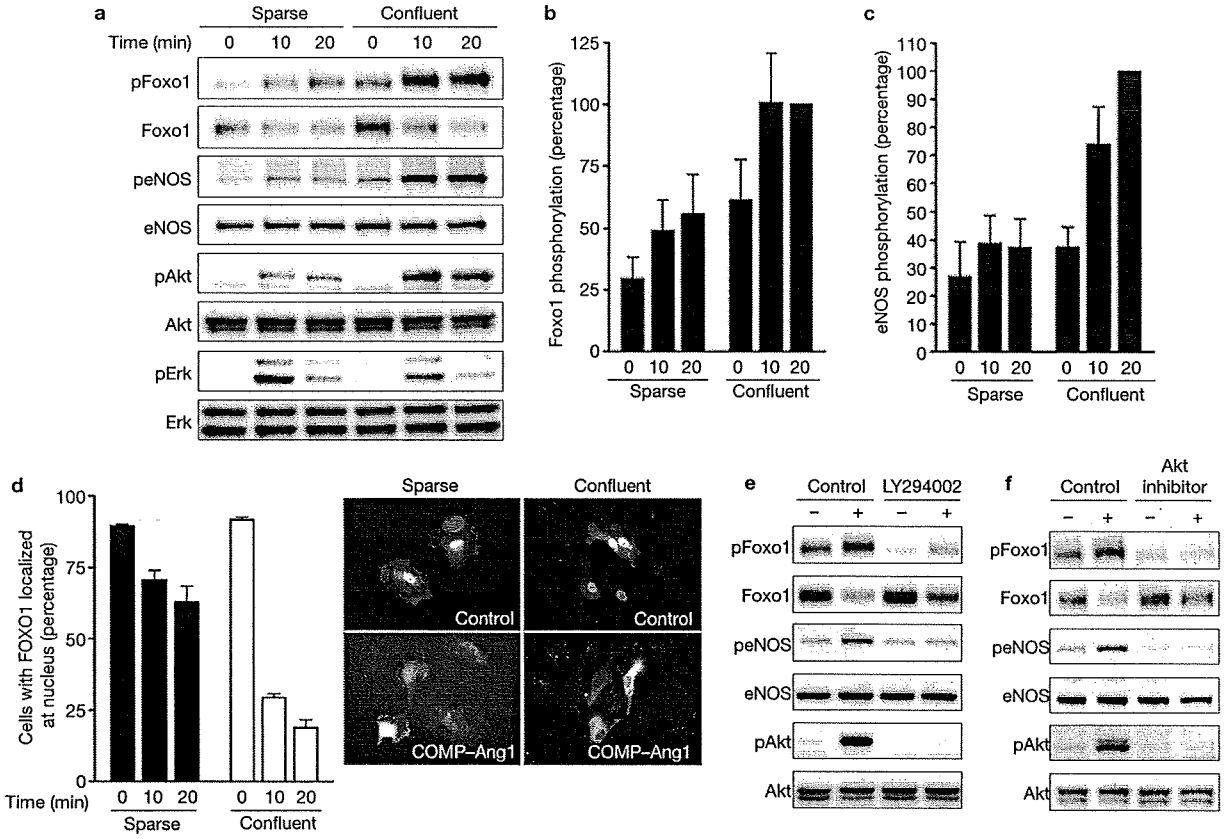

Figure 6 The presence of cell–cell contacts determines the preferential activation of Akt and subsequent phosphorylation of Foxo1 and eNOS. (**a**) Sparse and confluent HUVECs were starved and stimulated with COMP–Ang1. Cell lysates were analysed for phosphorylation of Foxo1, eNOS, Akt, and Erk. Note that Foxo1 and eNOS are more phosphorylated in the confluent cells than in the sparse cells. (**b**) COMP–Ang1–induced phosphorylation of Foxo1 observed in **a** was quantified. Foxo1 phosphorylation represents the ratio of phosphorylated Foxo1 to total Erk protein as a percentage of the ratio in the confluent cells stimulated for 20 min. Erk protein but not Foxo1 was used as normalization for protein loading, because anti-Foxo1 antibody does not recognize phosphorylated Foxo1. Values are expressed as means ± s.d. from seven independent experiments. (**c**) COMP–Ang1-induced phosphorylation of eNOS observed in **a** was quantified. eNOS phosphorylation represents the ratio of phosphorylated eNOS to total eNOS as a percentage of the ratio in the confluent cells stimulated for 20 min. Values are expressed as means ± s.d. from seven independent experiments. (**d**) Sparse and confluent HUVECs transfected with a plasmid encoding GFP–Foxo1 were starved for 6 h and stimulated with COMP–Ang1 for the time (min) as indicated. After fixation in methanol, the number of cells with GFP–Foxo1 localized at nucleus was counted and expressed as a percentage relative to total number of cells. At least 100 GFP-positive cells were scored for each treatment. Values are expressed as means ± s.d. from three independent experiments. Representative images of subcellular localization of GFP–Foxo1 in sparse (left) and confluent (right) cells are shown on the bottom. Upper and lower panels show the images in cells stimulated with vehicle or COMP–Ang1 for 20 min. (**e**, **f**) Confluent HUVECs were pre-treated with 20 μM LY294002 for 30 min (**e**) or 8 μM Akt inhibitor for 5 min (**f**) and subsequently stimulated with vehicle (–) or COMP–Ang1 (+) for 20 min. The effect of both inhibitors on COMP–Ang1-induced phosphorylation of Foxo1, eNOS, and Akt was examined. Uncropped images of **a**, **e**, and **f** are shown in Supplementary Information, Fig. S8.

Focal adhesion kinase (FAK) localizing at FCs and FAs mediates signalling by integrins and growth factor receptors to activate Erk[36,37]. Previously, it has been reported that Angl activates FAK to induce endothelial cell sprouting[13]. Thus, we tested the involvement of FAK in Erk activation downstream of cell–substratum contact-anchored Tie2 upon Angl stimulation. COMP–Angl induced tyrosine phosphorylation and accumulation of FAK to FCs in HUVECs (Fig. 5d and Supplementary Information, Fig. S7g) and increased the FAK-positive FC assembly as well as vinculin (Fig 5b, e). Consistent with the idea that the focal-adhesion-targeting domain of FAK (FAT) displaces FAK from FCs and FAs[36], overexpression of RFP-tagged FAT (RFP–FAT) perturbed the localization of FAK to FCs and FAs in HUVECs (Supplementary Information, Fig. S7h). Tie2 localization at peripheral cell–substratum contacts upon COMP–Angl stimulation was not influenced by overexpression of FAT (Supplementary Information, Fig. S7i). We next investigated the effect of FAT on Tie2-mediated intracellular signalling. Overexpression of GFP-tagged FAT (GFP–FAT) significantly but not completely inhibited COMP–Angl-induced Erk activation (Fig. 5f, g). In clear contrast, overexpression of FAT did not alter COMP–Angl-induced Akt activation (Fig. 5f, h). Furthermore, depletion of FAK by siRNAs partly inhibited COMP–Angl-induced Erk activation (Fig. 5i, j and Supplementary Information, Fig. S7j, k). Collectively, these results indicate that Erk activation by Tie2 anchored to cell–substratum contacts is ascribed partly to FAK.

Erk signalling is known to be involved in endothelial cell migration[38]. Thus, we examined the role of Erk in cell migration by Angl–Tie2 at cell–substratum contacts. Cell motility was enhanced when HUVECs

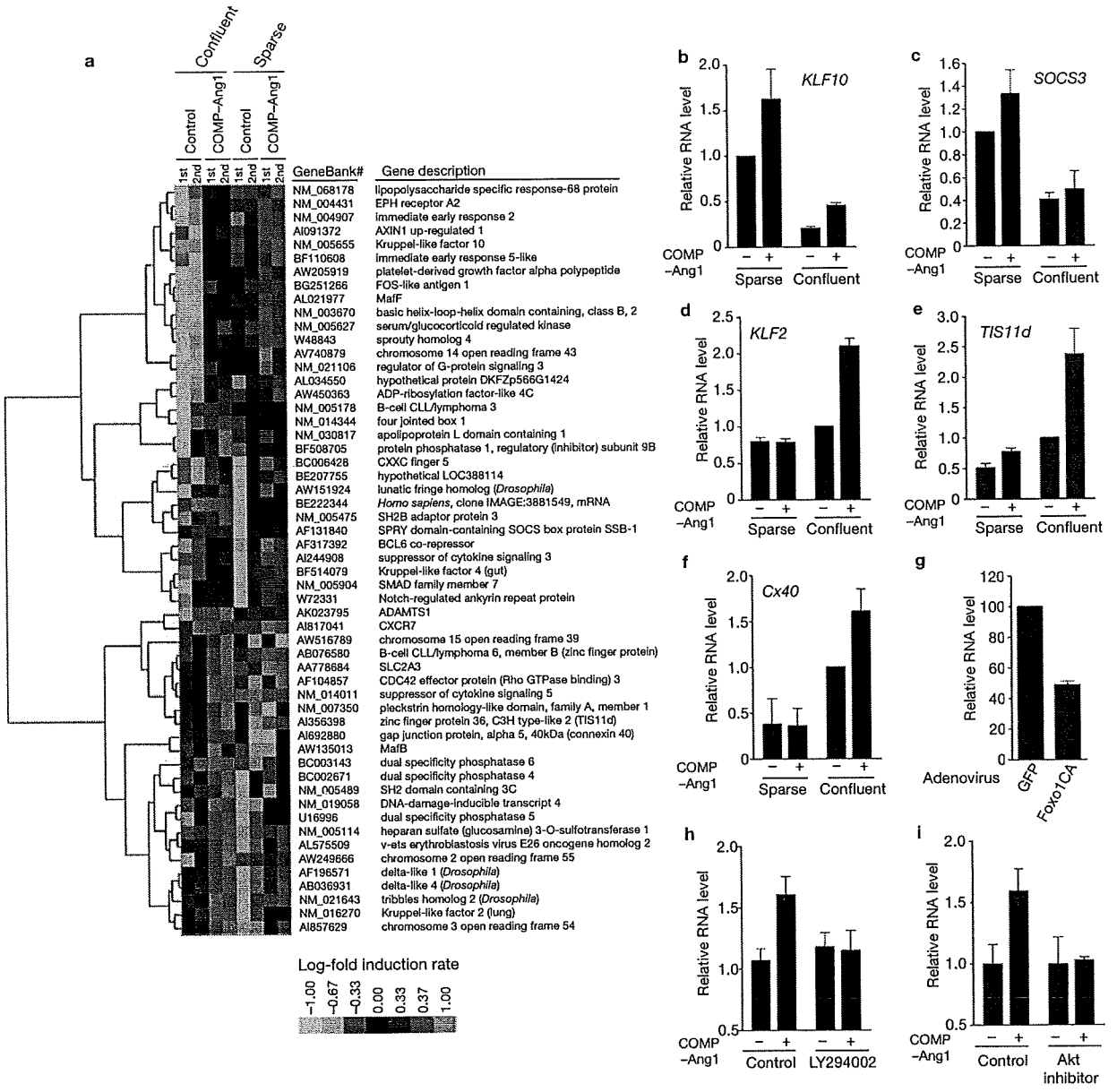

Figure 7 Ang1 stimulation leads to a distinct pattern of gene expression in HUVECs in the presence or absence of cell–cell contacts. (**a**) Total RNA was purified from confluent and sparse HUVECs stimulated with vehicle (control) or COMP–Ang1 for 1 h, and subjected to Affymetrix microarray analysis, as described in Methods. Genes corresponding to the criteria described in Methods were subjected to the cluster analysis. The results from two independent microarray analyses are displayed. Red and green represent higher and lower expression than the median for that particular gene, respectively. Color intensity is related to the difference with the median (black). (**b–f**) Total RNA was purified from confluent and sparse HUVECs stimulated with vehicle (–) or COMP–Ang1 (+) for 1 h, and expression levels of *KLF10* (**b**), *SOCS3* (**c**), *KLF2* (**d**), *TIS11d* (**e**) and *Cx40* (**f**) were analysed by real-time RT–PCR analysis as described in Supplementary Information, Methods. Bar graphs show relative RNA levels of each gene normalized to GAPDH levels. RNA levels are expressed relative to that in sparse (**b**, **c**) or confluent (**d–f**) cells stimulated with vehicle. Values are expressed as means ± s.d. from more than three independent experiments. (**g**) Total RNA was isolated from confluent HUVECs infected with adenovirus vectors encoding either GFP (GFP) or a constitutively active mutant of Foxo1 (Foxo1CA). Expression levels of *Cx40* were analysed as described for **f**, and expressed as a percentage relative to that in cells infected with GFP-encoding adenovirus vector. (**h**) Confluent HUVECs were stimulated with COMP–Ang1 in the presence (LY294002) or absence (control) of LY294002 as described in the legend of Fig. 6e. Expression levels of *Cx40* were analysed as described for **f**. Data are means ± s.d. of triplicate samples, and similar results were obtained in three independent experiments. (**i**) Confluent HUVECs were stimulated with COMP–Ang1 in the presence (Akt inhibitor) or absence (control) of Akt inhibitor as described in the legend of Fig. 6f. Expression levels of *Cx40* were analysed and expressed as described for **h**.

were placed on collagen- and COMP–Ang1-coated transwell filters, compared with cells adhering to collagen-coated filters. This enhanced cell motility was cancelled by inhibiting Erk using U0126, a MEK inhibitor (Fig. 5k, l). These findings suggest that Ang1–Tie2 at cell–substratum contacts regulates endothelial cell migration through the Erk signalling pathway.

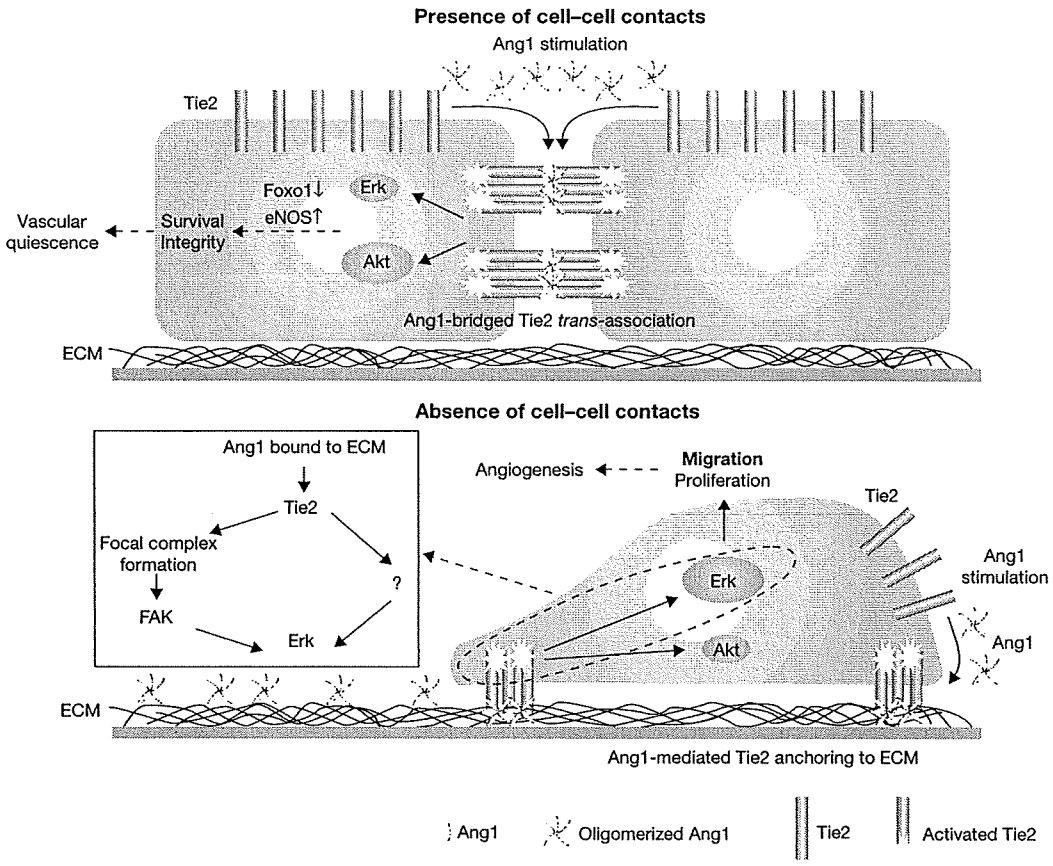

Figure 8 Schematic representation of a proposed model for how Ang1–Tie2 signalling is involved in both vascular quiescence and angiogenesis. (Upper panel) Under confluent conditions, oligomerized Ang1 bridges Tie2 at cell–cell contacts, resulting in formation of *trans*-association of Tie2. *Trans*-associated Tie2 at cell–cell contacts preferentially activates Akt–Foxo1 and Akt–eNOS signalling pathways, which may contribute to maintenance of vascular quiescence by enhancing endothelial survival and integrity (dashed arrows). (Lower panel) In the absence of cell–cell contacts, Tie2 forms a complex with ECM-bound Ang1 at cell–substratum contacts, which is different from focal adhesions, focal complexes and fibrillar adhesion. Ang1–Tie2 anchored to cell–substratum contacts preferentially activates the Erk pathway by inducing FAK-positive focal complex assembly. Ang1, therefore, seems to implicate FAK partly in the activation of Erk. This preferential activation of the Erk pathway induced by Ang1–Tie2 anchored to cell–substratum contacts may contribute to endothelial cell migration and proliferation, thereby promoting angiogenesis (dashed arrows). FC and ECM indicate focal complex and extracellular matrix, respectively.

The presence of cell–cell contacts determines preferential activation of Akt by Ang1 and subsequent phosphorylation of eNOS and Foxo1

Akt phosphorylates the forkhead transcription factor Foxo1 and endothelial nitric oxide synthase (eNOS), which play critical roles in endothelial functions[39,40]. To investigate the biological consequence of preferential activation of Akt by *trans*-associated Tie2, we examined Ang1-induced phosphorylation of Foxo1 and eNOS in the absence and presence of cell–cell contacts. Endothelial cell–cell contacts significantly enhanced COMP–Ang1-induced phosphorylation of Foxo1 and eNOS in HUVECs (Fig. 6a–c). Akt-dependent phosphorylation negatively regulates transcriptional activity of Foxo1 by promoting its nuclear exclusion. Consistently, nuclear export of Foxo1 by COMP–Ang1 was more prominent in confluent HUVECs than in sparse cells (Fig. 6d). Phosphatidylinositol-3 kinase (PI3K) inhibitor, LY294002, and Akt inhibitor impeded COMP–Ang1-induced phosphorylation of Foxo1 and eNOS (Fig. 6e, f). These findings indicate that phosphorylation of Foxo1 and eNOS mediated by PI3K–Akt are preferentially induced by *trans*-associated Tie2 compared to substratum-anchored Tie2.

Distinct gene expression profile in HUVECs upon Ang1 stimulation in the presence or absence of cell–cell contacts

To further clarify the consequence of Tie2 activation at cell–cell contacts and at cell–substratum contacts, we employed DNA microarray analyses. We carried out a global survey of mRNA in either confluent or sparse HUVECs upon COMP–Ang1 stimulation for 1 h. There was a striking difference in the induction of genes between confluent and sparse conditions (Fig. 7a). To confirm the microarray data, expression levels of several genes selectively induced under either sparse or confluent conditions were examined by quantitative real-time PCR analysis. Both basal expression and induction of *Krüppel-like factor (KLF) 10* and *suppressor of cytokine signaling 3 (SOCS3)* were greater in sparse cells than in confluent cells (Fig. 7b, c). In contrast,

KLF2, zinc finger protein 36, C3H type 2 (*TIS11d*), and *connexin40* (*Cx40*) were induced by COMP-Ang1 selectively in confluent cells (Fig. 7d, e, f). *Cx40*, the product of which is involved in intercellular communication, is known to be repressed by Foxo1 in endothelial cells [39]. Indeed, overexpression of a constitutively active mutant of Foxo1 decreased *Cx40* expression (Fig. 7g). Thus, we investigated whether a PI3K–Akt–Foxo1 signal axis is involved in COMP-Ang1-induced *Cx40* expression. LY294002 and Akt inhibitor prevented COMP-Ang1-induced *Cx40* induction in confluent cells (Fig. 7h, i). Collectively, these microarray analyses and real-time PCR validation clearly demonstrate a difference in induction of gene expression by Ang1 in the presence or absence of cell–cell contacts, and indicate that *trans*-associated Tie2 at cell–cell contacts regulates Foxo1-dependent gene expression through preferential activation of Akt.

DISCUSSION

Localization of Tie2 upon Ang1 stimulation depends upon the presence or absence of cell–cell contacts (Figs 1a, 3a). Tie2 localization at cell–cell contacts appears to be due to Ang1-bridged Tie2 *trans*-association. Tie2 activation at cell–cell contacts resulted in preferential activation of Akt, which in turn led to inhibition of Foxo1-mediated gene regulation and phosphorylation of eNOS. The Akt–Foxo1 pathway is known to be involved in Ang1-induced endothelial cell survival and blood vessel stability[39]. It has been also reported that the Akt–eNOS pathway is required for vascular maturation[40]. Thus, *trans*-associated Tie2 may contribute to maintenance of vascular quiescence through the Akt–Foxo1 and Akt–eNOS signalling pathways.

Ang1 also locates Tie2 to cell–substratum contacts that are different from FCs, FAs and FBs and preferentially activates Erk in the absence of cell–cell contacts. This Tie2 localization was resistant to detergent[27,28], indicating Tie2 is anchored to cell–substratum contacts. Moreover, Ang1 could bind to ECM such as fibronectin and collagen, as previously reported[41,42]. Upon being anchored to ECM by Ang1, Tie2 activated Erk partly through FAK. Formation of the Ang1–Tie2 complex at cell–substratum contacts accelerated FC formation (Fig. 5b, e), and probably vice versa, resulting in the implicating FAK in Ang1-induced Erk activation in isolated cells. This notion is consistent with recent reports revealing a role for FAK in vascular development[43,44].

During angiogenesis, endothelial cells sprouting from the pre-existing blood vessels lose cell–cell adhesion and need to proliferate and migrate to form neovasculature. Erk is responsible for endothelial proliferation and migration during angiogenesis[38,45]. Inhibition of Erk resulted in decreased migration by substratum-anchored Ang1. As several lines of evidence suggest that Tie2 signalling mediates pathological and physiological angiogenesis[14,15,17–20], Ang1–Tie2–ECM complexes at cell–substratum contacts may accelerate angiogenesis by promoting proliferation and migration of isolated endothelial cells. However, regulation of angiogenesis by Ang1–Tie2 might be more complex, since it has been reported that Tie2 is expressed in stalk cells, but not in tip cells, which proliferate and migrate during angiogenesis[46]. Thus, further investigation is required to resolve this mechanism.

We propose that *trans*-associated Tie2 bridged by Ang1 and cell–substratum contact-anchored Tie2 by Ang1 might be preferable for vascular quiescence and for angiogenesis via Akt and Erk activation, respectively (Fig. 8). □

Note added in proof: a related manuscript by Saharinen et al. *(*Nature Cell Biol. *10, 527–537; doi:10.1038/ncb1715; 2008) is also published in this issue.*

METHODS

Immunocytochemistry and fluorescence imaging. HUVECs and CHO cells grown on a collagen-coated glass-base dish (Asahi Techno Glass Corporation, Chiba, Japan) were transfected with expression plasmids encoding Tie2–GFP, Tie2Δcyto–GFP, Tie2Δcyto–HA, RFP–Crk, GFP–tensin and RFP–FAT as indicated in the figures. HUVECs starved for 3 h in medium 199 containing 0.5% BSA and CHO cells in Dulbecco's modified Eagle's medium (DMEM)/F12 nutrient mixture (Sigma-Aldrich, St. Louis, MO) were stimulated for the time periods as indicated in the figures. After stimulation, the cells were fixed in PBS containing 2% formaldehyde for 30 min at 4 °C, washed with PBS, and permeabilized with 0.05% Triton X-100 for 30 min at 4 °C. To examine the detergent insolubility of Tie2–GFP anchoring to the substratum, the cells were washed with PBS, and extracted in 0.5% Triton X-100 in cytoskeleton stabilizing buffer containing 10 mM PIPES at pH 6.8, 300 mM sucrose, 100 mM NaCl, 3 mM $MgCl_2$, 1 mM EGTA and 1 x protease inhibitor cocktail (Roche Applied Science, Indianapolis, IN) for 3 min at room temperature (RT). After washing with PBS, the cells were fixed with 2% formaldehyde in PBS for 30 min at 4 °C. Cells were blocked with PBS containing 4% BSA for 1 h at RT and immunostained with anti-Tie2, anti-VE-cadherin, anti-HA, anti-FLAG, anti-vinculin, anti-α5 integrin, anti-β3 integrin, anti-PECAM-1, anti-VASP, anti-talin, anti-fibronectin, anti-phosphoTie2, and anti-FAK antibodies for 1 h at RT and with rhodamine-phalloidin for 20 min at RT. Protein reacting with antibody was visualized with species-matched Alexa 488- or Alexa 546-labelled secondary antibodies. Fluorescence images of GFP, RFP, rhodamine, Alexa 488 and Alexa 546 were recorded with an Olympus IX-81 inverted fluorescence microscope (Olympus Corporation, Tokyo, Japan) with a cooled CCD camera CoolSNAP-HQ (Roper Scientific, Tucson, AZ), and appropriate filter sets for GFP, Alexa 488 and Alexa 546, and with a FluoView FV1000 confocal microscope (Olympus Corporation) with a 60x oil immersion objective lens. HUVECs and CHO cells transfected with plasmids expressing fluorescently tagged proteins (GFP, HcRed, and RFP) were time-lapse imaged on an Olympus IX-81 inverted fluorescence microscope as described previously [47,48].

***In vitro* Ang1-bridged Tie2 association assay.** To produce recombinant sTie2–HA protein (extracellular domain of Tie2 tagged with HA), 293F cells were transfected with pcDNA3.1-sTie2–HA vector, and cultured in Free Style 293 expression media for 7 days. sTie2–HA protein secreted into the medium was collected every 2 days, and incubated with ProBond resin (Invitrogen Corp., Carlsbad, CA) overnight at 4 °C. sTie2–HA protein bound to the beads was eluted with 500 mM imidazole, concentrated with Amicon Centriplus (Millipore, Billerica, MA), and buffer exchanged into PBS by dialysis.

Ang1-bridged Tie2 association was analysed as described in Supplementary Information Fig. S3a. Initially, protein G sepharose beads (GE Healthcare Life Science, Piscataway, NJ) were incubated with 0.1 μg of Fc, sTie1–Fc or sTie2–Fc protein in binding buffer (50 mM Tris-HCl at pH 7.5, 100 mM NaCl, 0.02% Triton X-100) for 2 h at 4 °C, washed three times with binding buffer, and incubated with 1 μg of Ang1 or its variants (COMP–Ang1, GCN4–Ang1 and MAT–Ang1) for 2 h at 4 °C. The beads were extensively washed with binding buffer four times, and subsequently incubated with 3 μg of sTie2–HA protein for 2 h at 4 °C. After washing, the precipitates were subjected to Western blot analysis with anti-Flag and anti-HA antibodies to quantify the co-precipitated Ang1 and its variants and sTie2–HA protein, respectively. Proteins reacting with primary antibodies were visualized by the ECL system (GE Healthcare Life Science) for detecting peroxidase-conjugated secondary antibodies and analysed with an LAS-1000 system (Fuji Film, Tokyo, Japan).

Cell aggregation and *in vivo* Tie2 *trans*-association assays. Suspension 293F cells transfected with the plasmids expressing GFP, Tie2–GFP, Tie2Δcyto–GFP, Tie2KD–GFP, or VEGFR2 plus IRES-driven GFP were suspended in Free Style 293 expression media and placed on 6 well-plates in a density of 5.0×10^5 cells per well (1 ml per well). Then, the cells were agitated for 4 h using a gyratory shaker in the presence of vehicle, Ang1, COMP–Ang1 or VEGF. After the incubation, the phase-contrast and the fluorescence images were recorded by Olympus IX-81 inverted fluorescence microscope. The differential interference contrast (DIC) and the fluorescence images were also obtained with a FluoView

FV1000 confocal microscope. The numbers of cell aggregates including more than 4 cells were counted in, at least, 10 different fields. The size of cell aggregates was measured using MetaMorph 6.1 software.

For the *in vivo* Tie2 *trans*-association assay, 293F cells transfected with the vectors encoding either GFP, Tie2Δcyto–GFP, or Tie2Δcyto–HA were washed and resuspended in DMEM in a density of 10^6 cells per ml. The cells expressing Tie2Δcyto–HA were mixed with either those expressing Tie2Δcyto–GFP or those expressing GFP in a 6 well-plate (2 x 10^6 cells $well^{-1}$). The cell suspensions were agitated for 1 h in the presence or absence of 400 ng ml^{-1} COMP–Ang1. After the incubation, the cells were collected in a 15 ml-conical tube, washed with ice-cold PBS and lysed at 4°C in lysis buffer containing 50 mM Tris-HCl at pH 7.5, 150 mM NaCl, 0.5% Triton X-100 and 1 x protease inhibitor cocktail. BaF–Tie2Δcyto–HA cells (1.5 x 10^6 cells) were also mixed with either BaF3 cells (1.5 x 10^6 cells) or BaF–Tie2Δcyto–GFP cells (1.5 x 10^6 cells) in RPMI1640 (Nissui, Tokyo, Japan) supplemented with 2 ng ml^{-1} murine IL3, and stimulated with or without 400 ng ml^{-1} COMP–Ang1 for 5 h. After the incubation, the cells were washed with ice-cold PBS and lysed as described above. Precleared cell lysates were subjected to immunoprecipitaion with anti-GFP antibody followed by immunoblot analysis with anti-HA antibody.

Microarray analysis. Confluent and sparse HUVECs on a collagen-coated dish were starved in HuMedia-EB2 medium (Kurabo, Kurashiki, Japan) containing 0.5% fetal calf serum (FCS) for 15 h, and stimulated with vehicle or COMP–Ang1 (200 ng ml^{-1}) for 1 h. After the stimulation, total RNAs were purified from the pooled RNA of triplicate samples using Trizol reagent (Invitrogen Corp.) and reverse-transcribed to cDNAs. Biotin-labelled RNAs derived from cDNAs were fragmented according to the manufacturer's instructions (Affymetrix, Santa Clara, CA). Labelled cRNA probes were hybridized to Affymerix U133plus 2.0 array (Affymetrix). The microarray data scanned through an Affymetrix GeneChip scanner 3000 7G were globally normalized by Affymetrix Microarray Suite 5.0 software and were scaled to a target intensity of 100. Microarray analysis was performed in duplicate from independent RNA preparations. Data were analysed according to the minimum information about a microarray experiment (MIAME) rule. To identify the genes regulated by Ang1–Tie2 signal, we picked up the genes which fulfill the two criteria: (1) the hybridization signal after COMP–Ang1 stimulation was higher than 80 in duplicate experiments and (2) the induction was greater than 1.5-fold under either confluent or sparse conditions upon COMP–Ang1 stimulation in duplicate experiments. The genes that conformed to the two criteria were further clustered on the basis of similar regulation patterns using Gene cluster (created by M. B. Eisen, University od California, Berkeley, CA) and Java Tree View software according to the manual on the default settings. The complete microarray data sets are available from the Gene Expression Omnibus (GSE9677).

Note: Supplementary Information is available on the Nature Cell Biology website.

ACKNOWLEDGEMENTS

We are grateful to T. Suda (Keio University, Tokyo, Japan) for the Tie2 cDNA, to A. Fukamizu (University of Tsukuba, Tsukuba, Japan) for the Foxo1 cDNA, to K.M. Yamada (National Institute of Health) for GFP–tensin, to J. Nakae (Kobe University Graduate School of Medicine, Kobe, Japan) for the adenovirus encoding Foxo1 mutant, to A. Mizushima, M. Sone, M. Maeoka, and Y. Matsuura for technical assistance, to M. Masuda, H. Hanada, and S. Yamanoto for helpful advice and to J.T. Pearson and J.S. Gutkind for critical reading of the manuscript. This work was supported in part by grants from the Ministry of Education, Science, Sports and Culture of Japan; the Ministry of Health, Labour, and Welfare of Japan; and the Program for the Promotion of Fundamental Studies in Health Sciences of the National Institute of Biomedical Innovation (to S.F., T.M, T.K. N.M.); the Naito Foundation (to S.F.); Takeda Medical Research Foundation (to N.M); and KOSEF through the NRL Program (2004-02376 to G.Y.K) funded by the MOST.

AUTHOR CONTRIBUTIONS

S. F. and N. M. designed and wrote the paper. S. F. performed the all cell biological and biochemical analysis. K. S. and K. N. helped with the experiments performed by S. F. T. M. and T. K. performed microarray analyses. M. S. and N. T. helped with VEGF-related and Tie2–BaF experiments. H. Z. K. and G. Y. K. prepared several forms of recombinant Ang1.

COMPETING FINANCIAL INTERESTS

The authors declare no competing financial interests.

Published online at http://www.nature.com/naturecellbiology/
Reprints and permissions information is available online at http://npg.nature.com/reprintsandpermissions/

1. Yancopoulos, G. D. *et al.* Vascular-specific growth factors and blood vessel formation. *Nature* **407**, 242–248 (2000).
2. Mammoto, T. *et al.* Angiopoietin-1 requires p190RhoGAP to protect against vascular leakage *in vivo*. *J. Biol. Chem.* **282**, 23910–23918 (2007).
3. Jho, D. *et al.* Angiopoietin-1 opposes VEGF-induced increase in endothelial permeability by inhibiting TRPC1-dependent Ca2 influx. *Circ. Res.* **96**, 1282–1290 (2005).
4. Brindle, N. P., Saharinen, P. & Alitalo, K. Signaling and functions of angiopoietin-1 in vascular protection. *Circ. Res.* **98**, 1014–1023 (2006).
5. Baffert, F., Le, T., Thurston, G. & McDonald, D. M. Angiopoietin-1 decreases plasma leakage by reducing number and size of endothelial gaps in venules. *Am. J. Physiol. Heart Circ. Physiol.* **290**, H107-H118 (2005).
6. Gamble, J. R. *et al.* Angiopoietin-1 is an antipermeability and anti-inflammatory agent *in vitro* and targets cell junctions. *Circ. Res.* **87**, 603–607 (2000).
7. Cho, C. H. *et al.* Designed angiopoietin-1 variant, COMP-Ang1, protects against radiation-induced endothelial cell apoptosis. *Proc. Natl Acad. Sci.USA* **101**, 5553–5558 (2004).
8. Kwak, H. J., So, J. N., Lee, S. J., Kim, I. & Koh, G. Y. Angiopoietin-1 is an apoptosis survival factor for endothelial cells. *FEBS Lett.* **448**, 249–253 (1999).
9. Papapetropoulos, A. *et al.* Angiopoietin-1 inhibits endothelial cell apoptosis via the Akt/Survivin pathway. *J. Biol. Chem.* **275**, 9102–9105 (2000).
10. Thurston, G. *et al.* Angiopoietin-1 protects the adult vasculature against plasma leakage. *Nature Med.* **6**, 460–463 (2000).
11. Thurston, G. *et al.* Leakage-resistant blood vessels in mice transgenically overexpressing angiopoietin-1. *Science* **286**, 2511–2514 (1999).
12. Master, Z. *et al.* Dok-R plays a pivotal role in angiopoietin-1-dependent cell migration through recruitment and activation of Pak. *EMBO J.* **20**, 5919–5928 (2001).
13. Kim, I. *et al.* Angiopoietin-1 induces endothelial cell sprouting through the activation of focal adhesion kinase and plasmin secretion. *Circ. Res.* **86**, 952–959 (2000).
14. Cho, C. H. *et al.* COMP-Ang1: A designed angiopoietin-1 variant with nonleaky angiogenic activity. *Proc. Natl Acad. Sci. USA* **101**, 5547–5552 (2004).
15. Asahara, T. *et al.* Tie2 receptor ligands, angiopoietin-1 and angiopoietin-2, modulate VEGF-induced postnatal neovascularization. *Circ. Res.* **83**, 233–240 (1998).
16. Yoon, M. J. *et al.* Localization of Tie2 and phospholipase D in endothelial caveolae is involved in angiopoietin-1-induced MEK/ERK phosphorylation and migration in endothelial cells. *Biochem. Biophys. Res. Commun.* **308**, 101–105 (2003).
17. Lin, P. *et al.* Inhibition of tumor angiogenesis using a soluble receptor establishes a role for Tie2 in pathologic vascular growth. *J. Clin. Invest.* **100**, 2072–2078 (1997).
18. Lin, P. *et al.* Antiangiogenic gene therapy targeting the endothelium-specific receptor tyrosine kinase Tie2. *Proc. Natl Acad. Sci. USA* **95**, 8829–8834 (1998).
19. Peters, K. G. *et al.* Functional significance of Tie2 signaling in the adult vasculature. *Recent Prog. Horm. Res.* **59**, 51–71 (2004).
20. Wong, A. L. *et al.* Tie2 expression and phosphorylation in angiogenic and quiescent adult tissues. *Circ. Res.* **81**, 567–574 (1997).
21. Carmeliet, P. *et al.* Targeted deficiency or cytosolic truncation of the VE-cadherin gene in mice impairs VEGF-mediated endothelial survival and angiogenesis. *Cell* **98**, 147–157 (1999).
22. Zanetti, A. *et al.* Vascular endothelial growth factor induces SHC association with vascular endothelial cadherin: a potential feedback mechanism to control vascular endothelial growth factor receptor-2 signaling. *Arterioscler. Thromb. Vasc. Biol.* **22**, 617–622 (2002).
23. Lampugnani, M. G., Orsenigo, F., Gagliani, M. C., Tacchetti, C. & Dejana, E. Vascular endothelial cadherin controls VEGFR-2 internalization and signaling from intracellular compartments. *J. Cell Biol.* **174**, 593–604 (2006).
24. Zaidel-Bar, R., Cohen, M., Addadi, L. & Geiger, B. Hierarchical assembly of cell-matrix adhesion complexes. *Biochem. Soc. Trans.* **32**, 416–420 (2004).
25. Geiger, B., Bershadsky, A., Pankov, R. & Yamada, K. M. Transmembrane crosstalk between the extracellular matrix--cytoskeleton crosstalk. *Nature Rev. Mol. Cell Biol* **2**, 793–805 (2001).
26. Cascone, I., Napione, L., Maniero, F., Serini, G. & Bussolino, F. Stable interaction between α5β1 integrin and Tie2 tyrosine kinase receptor regulates endothelial cell response to Ang-1. *J. Cell Biol.* **170**, 993–1004 (2005).
27. Wulfkuhle, J. D. *et al.* Domain analysis of supervillin, an F-actin bundling plasma membrane protein with functional nuclear localization signals. *J. Cell Sci.* **112**, 2125–2136 (1999).
28. Adams, C. L., Nelson, W. J. & Smith, S. J. Quantitative analysis of cadherin-catenin-actin reorganization during development of cell-cell adhesion. *J. Cell Biol.* **135**, 1899–1911 (1996).
29. Kim, I. *et al.* Angiopoietin-1 regulates endothelial cell survival through the phosphatidylinositol 3'-Kinase/Akt signal transduction pathway. *Circ. Res.* **86**, 24–29 (2000).
30. Kanda, S., Miyata, Y., Mochizuki, Y., Matsuyama, T. & Kanetake, H. Angiopoietin 1 is mitogenic for cultured endothelial cells. *Cancer Res.* **65**, 6820–6827 (2005).
31. Teichert-Kuliszewska, K. *et al.* Biological action of angiopoietin-2 in a fibrin matrix model of angiogenesis is associated with activation of Tie2. *Cardiovasc. Res.* **49**, 659–670 (2001).
32. Weber, C. C. *et al.* Effects of protein and gene transfer of the angiopoietin-1 fibrinogen-like receptor-binding domain on endothelial and vessel organization. *J. Biol. Chem.* **280**, 22445–22453 (2005).

33. Dallabrida, S. M., Ismail, N., Oberle, J. R., Himes, B. E. & Rupnick, M. A. Angiopoietin-1 promotes cardiac and skeletal myocyte survival through integrins. *Circ. Res.* **96,** e8-24 (2005).
34. Aplin, A. E., Short, S. M. & Juliano, R. L. Anchorage-dependent regulation of the mitogen-activated protein kinase cascade by growth factors is supported by a variety of integrin α chains. *J. Biol. Chem.* **274,** 31223–31228 (1999).
35. Short, S. M., Talbott, G. A. & Juliano, R. L. Integrin-mediated signaling events in human endothelial cells. *Mol. Biol. Cell* **9,** 1969–1980 (1998).
36. Schlaepfer, D. D. & Mitra, S. K. Multiple connections link FAK to cell motility and invasion. *Curr. Opin. Genet. Dev.* **14,** 92–101 (2004).
37. Parsons, J. T. Focal adhesion kinase: the first ten years. *J. Cell Sci.* **116,** 1409–1416 (2003).
38. Eliceiri, B. P., Klemke, R., Stromblad, S., & Cheresh, D. A. Integrin αV β3 requirement for sustained mitogen-activated protein kinase activity during angiogenesis. *J. Cell Biol.* **140,** 1255–1263 (1998).
39. Daly, C. *et al.* Angiopoietin-1 modulates endothelial cell function and gene expression via the transcription factor FKHR (FOXO1). *Genes Dev.* **18,** 1060–1071 (2004).
40. Chen, J. *et al.* Akt1 regulates pathological angiogenesis, vascular maturation and permeability in vivo. *Nature Med.* **11,** 1188–1196 (2005).
41. Xu, Y. & Yu, Q. Angiopoietin-1, unlike angiopoietin-2, is incorporated into the extracellular matrix via its linker peptide region. *J. Biol. Chem.* **276,** 34990–34998 (2001).
42. Carlson, T. R., Feng, Y., Maisonpierre, P. C., Mrksich, M. & Morla, A. O. Direct cell adhesion to the angiopoietins mediated by integrins. *J. Biol. Chem.* **276,** 26516–26525 (2001).
43. Braren, R. *et al.* Endothelial FAK is essential for vascular network stability, cell survival, and lamellipodial formation. *J. Cell Biol.* **172,** 151–162 (2006).
44. Shen, T. L. *et al.* Conditional knockout of focal adhesion kinase in endothelial cells reveals its role in angiogenesis and vascular development in late embryogenesis. *J. Cell Biol.* **169,** 941–952 (2005).
45. Meadows, K. N., Bryant, P. & Pumiglia, K. Vascular endothelial growth factor induction of the angiogenic phenotype requires Ras activation. *J. Biol. Chem.* **276,** 49289–49298 (2001).
46. Yana, I. *et al.* Crosstalk between neovessels and mural cells directs the site-specific expression of MT1-MMP to endothelial tip cells. *J. Cell Sci.* **120,** 1607–1614 (2007).
47. Nagashima, K. *et al.* Adaptor protein Crk is required for ephrin-B1-induced membrane ruffling and focal complex assembly of human aortic endothelial cells. *Mol. Biol. Cell* **13,** 4231–4242 (2002).
48. Sakurai, A. *et al.* MAGI-1 is required for Rap1 activation upon cell-cell contact and for enhancement of vascular endothelial cadherin-mediated cell adhesion. *Mol. Biol. Cell* **17,** 966–976 (2006).